

UNCLASSIFIED

AD NUMBER

AD833881

LIMITATION CHANGES

TO:

Approved for public release; distribution is unlimited.

FROM:

Distribution authorized to U.S. Gov't. agencies and their contractors; Critical Technology; MAR 1968. Other requests shall be referred to Army Electronics Command, AMSEL-KL-TG, Fort Monmouth, NJ 07703. This document contains export-controlled technical data.

AUTHORITY

usaec ltr, 16 jun 1971

THIS PAGE IS UNCLASSIFIED

SU-IPR Report No. 233



TECHNICAL REPORT ECOM-02041-13

Some Studies of Whistler Instability

AD8333881

by

F.W. Crawford

J.C. Lee

J.A. Tataronis

MARCH 1968

D D C
RECORDED
JUN 17 1968
R
REGISTRATION
D

This document is subject to special export controls and each transmittal to foreign governments or foreign nationals may be made only with prior approval of CG, USAECOM, Attn: AMSEL-KL-TG, Ft. Monmouth, N.J. 07703

ECOM

UNITED STATES ARMY ELECTRONICS COMMAND • FORT MONMOUTH, N.J.
CONTRACT DA-28-043 AMC-02041(E) and NASA Grant NGR-05-020-176



INSTITUTE FOR PLASMA RESEARCH
STANFORD UNIVERSITY, STANFORD, CALIFORNIA

DISCLAIMER NOTICE

**THIS DOCUMENT IS THE BEST
QUALITY AVAILABLE.**

**COPY FURNISHED CONTAINED
A SIGNIFICANT NUMBER OF
PAGES WHICH DO NOT
REPRODUCE LEGIBLY.**

SOME STUDIES OF WHISTLER INSTABILITY

by

F. W. Crawford, J. C. Lee and J. A. Tataronis

NASA Grant NGR 05-020-176
and
US Army Electronics Command
Contract DA 28-043 AMC-02041(E)

SU-IPR Report No. 233
March 1968

[To be presented at: NATO Advanced Study Institute on
Plasma Waves in Space and in the Laboratory, Røros,
Norway, April 1968.]

Institute for Plasma Research
Stanford University
Stanford, California

CONTENTS

	<u>Page</u>
ABSTRACT	1
1. INTRODUCTION	2
2. BASIC DISPERSION RELATIONS	3
3. NUMERICAL SOLUTIONS OF THE DISPERSION RELATION	6
3.1 Zero Plasma and Beam Temperatures	6
3.2 Nonzero Plasma Temperature. Zero Beam Temperature	7
3.3 Zero Plasma Temperature. Nonzero Beam Temperature	9
4. INSTABILITY CLASSIFICATION	10
4.1 Zero Plasma and Beam Temperatures	11
4.2 Effect of Collisions	12
4.3 Effect of Plasma Temperature	12
4.4 Effect of Beam Temperature	13
5. COMPETING INSTABILITIES	14
5.1 Cyclotron Harmonic Waves ($k_{\parallel} = 0$)	14
5.2 Longitudinal Beam/Plasma Interaction ($k_{\perp} = 0$)	17
6. DISCUSSION	21
ACKNOWLEDGEMENTS	22
REFERENCES	23

LIST OF FIGURES

	<u>Page</u>
1. Whistler Instabilities: Mode Coupling for Zero Plasma and Beam Temperatures [$(\omega_p^2/\omega_c^2) = 25$, $(\omega_b^2/\omega_c^2) = 1$, $(v_{0\parallel}/c) = -0.05$]	25
2. Effect of Nonzero Plasma Temperature on the Unstable Mode of Fig. 1(c) [$(\omega_p^2/\omega_c^2) = 25$, $(\omega_b^2/\omega_c^2) = 1$, $(v_{0\parallel}/c) = -0.05$, $(\langle v_\perp^2 \rangle^{1/2}/c) = 0.025$]	26
3. Effect of Nonzero Beam Temperature on the Unstable Mode of Fig. 1(c) [$(\omega_p^2/\omega_c^2) = 25$, $(\omega_b^2/\omega_c^2) = 1$, $(v_{0\parallel}/c) =$ -0.05 , $(\langle v_\perp^2 \rangle^{1/2}/c) = 0.025$]	27
4. Absolute and Convective Instabilities	28
5. Stability Analysis: k-Plane Plot [$(\omega_p^2/\omega_c^2) = 25$, $(\omega_b^2/\omega_c^2) = 1$, $(\langle v_\perp^2 \rangle^{1/2}/c) = 0.025$, $(v_{0\parallel}/c) = -0.05$].	29
6. Stability Analysis: Loci of Branch-Points in the Com- plex ω -Plane [$(\omega_p^2/\omega_c^2) = 25$, $(\omega_b^2/\omega_c^2) = 1$]	30
7. Stability Analysis: Loci of Branch-Points in the ω -Plane, and Saddle-Points in the k-Plane, with varying (ω_b^2/ω_c^2) [$(\omega_p^2/\omega_c^2) = 25$, $(v_{0\parallel}/c) = -0.05$, $(\langle v_\perp^2 \rangle^{1/2}/c) = 0.025$]	31
8. Stability Analysis: Effect of Collisions [$(\omega_p^2/\omega_c^2) = 25$, $(\omega_b^2/\omega_c^2) = 1$, $(v_{0\parallel}/c) = -0.05$]	32, 33
9. Stability Analysis: Effect of Plasma Temperature [$(\omega_p^2/\omega_c^2) = 25$, $(\omega_b^2/\omega_c^2) = 1$, $(v_{0\parallel}/c) = -0.05$]	34
10. Stability Analysis: Effect of Beam Temperature [$(\omega_p^2/\omega_c^2) = 25$, $(\omega_b^2/\omega_c^2) = 1$, $(v_{0\parallel}/c) = -0.05$]	35
11. Dispersion Characteristics for Perpendicularly Propa- gating Cyclotron Harmonic Waves: Maxwellian Electron Velocity Distribution	36

LIST OF FIGURES (Continued)

	<u>Page</u>
12. Dispersion Characteristics for Perpendicularly Propagating Cyclotron Harmonic Waves: Ring Electron Velocity Distribution	37
13. Criteria for the Onset of Instability for Perpendicularly Propagating Cyclotron Harmonic Waves in a Mixture of (α) Maxwellian, and $(1-\alpha)$ Ring Electron Velocity Distributions.	38, 39
14. Maximum Instability Growth Rates for a Mixture of Maxwellian and Ring Electron Velocity Distributions . . .	40

SOME STUDIES OF WHISTLER INSTABILITY

by

F. W. Crawford, J. C. Lee and J. A. Tataronis

Institute for Plasma Research
Stanford University
Stanford, California

ABSTRACT

This paper treats the instability excited when a transverse electromagnetic plasma wave, propagating in the right-hand polarized (whistler) mode parallel to a uniform magnetic field, interacts with a stream of monoenergetic gyrating electrons. The objectives of the work are two-fold, first to obtain numerical estimates of the growth rates for various parameters, and second to identify the instabilities as being either absolute or convective. The results show that if the background plasma temperature is zero, absolute instability, i.e. temporal growth, always occurs. This instability may be quenched either by collisions or nonzero electron temperature in the background plasma, leaving a convective instability, i.e. spatial amplification. The absolute instability can also be quenched by introducing a longitudinal energy spread in the beam. Even when whistler growth is predicted theoretically, it may not be observable in practice, due to the presence of competing instabilities. Two of these are treated in the paper: perpendicularly propagating cyclotron harmonic waves, and longitudinal beam/plasma interaction.

1. INTRODUCTION

Whistler instability is of interest in areas as widely separated as magnetospheric physics, thermonuclear fusion, and microwave beam plasma amplification. There are consequently many descriptions of it to be found in the literature, written from differing points of view, and covering numerous special charged particle velocity distributions.¹⁻¹² In this paper, we present results of an extensive series of computations on variations of the basic case of a gyrating electron beam interacting with a cold background plasma. Only propagation parallel to the magnetic field will be considered. A particular feature of the work, lacking from most previous studies, is a detailed stability analysis to determine whether the instabilities are such as to give wave growth in space (convective) or time (absolute).^{13,14} In addition, potential competing instabilities have been examined so that their growth rates can be compared with that in the whistler mode for the same parameters.

The plan of the paper is as follows. In Section 2, we present the dispersion relation for a Maxwellian plasma penetrated by an electron beam with both longitudinal and transverse energy spread. Numerical solutions for several limiting cases of this dispersion relation are examined in Section 3 for real wave-number and complex frequency, and predict the occurrence of instability. The nature of this instability is discussed in Section 4, where it is shown that in some parameter ranges temporal wave growth occurs, and in others spatial growth. Competing instabilities are treated in Section 5, and the paper concludes with a brief discussion of the results and their implications in Section 6.

2. BASIC DISPERSION RELATIONS

In what follows, the whistler mode is defined as a right-handed polarized electromagnetic magnetoplasma wave, propagating at angle $\theta \approx 90^\circ$ parallel to the static magnetic field with phase velocity (ω/c) , where c is the speed of light, and $(\omega_c) \ll 1$, where ω_c is the electron gyrofrequency. It will be assumed that (ω_c) is high enough for ion motions to be ignored. The analysis of plasma wave propagation is now highly developed, and as far as infinite homogeneous plasmas immersed in a constant magnetic field are concerned, the derivation of dispersion relations has been reduced to the mechanical process of substituting steady-state velocity distributions for the charged particles into a standard expression derived by combining the collisionless Boltzmann equation with Maxwell's equations. For the whistler, the generalized dispersion relation is given by^{15,16}

$$D(\omega, k) \equiv c^2 k^2 - \omega^2 + \sum \omega_p^2 \int_{-\infty}^{+\infty} dv_{||} \int_0^{\infty} dv_{\perp} 2\pi v_{\perp} f_0(v_{||}, v_{\perp}) \\ \times \left[\frac{\omega - kv_{||}}{\omega - kv_{||} - \omega_c} + \frac{k^2 v_{\perp}^2}{2(\omega - kv_{||} - \omega_c)^2} \right] = 0 . \quad (1)$$

In this expression, the summation is taken over all beam and plasma electron components; ω_p is the plasma frequency; $f_0(v_{||}, v_{\perp})$ is the steady state velocity distribution, and $v_{||}$ and v_{\perp} are the components of the velocity vector parallel and perpendicular to the magnetic field, respectively. Equation (1) is defined for $\omega_i < 0$. For $\omega_i \geq 0$, its analytic continuation must be used. Here subscript i denotes the imaginary component of $\omega (\equiv \omega_r + i\omega_i)$.

We now specialize Eq. (1) to the case of stationary plasma with an isotropic Maxwellian electron velocity distribution, $f_p(v_{||}, v_{\perp})$ and a stream of gyrating electrons with velocity distribution, $f_b(v_{\perp}, v_{||} - v_{0||})$.

where ϵ_0 is the dielectric constant of the beam, v_{\perp} is the transverse speed of the beam, e is the electron charge, m_e is the mass of the electron, ω_b is the beam electrons' gyrofrequency, ω_c is the cyclotron frequency of the beam electrons, ω_{pe} is the plasma frequency, and $\omega_{pe}^2 = \omega_b^2 + \omega_c^2$. The value of the beam electrons' gyrofrequency can be the normalized:

$$\frac{\omega_b}{\omega_c} = \int_0^\infty v_{\perp}^2 f(v_{\perp}) dv_{\perp} = 1 \quad (2)$$

Substituting Eq. (2) in Eq. (1), and integrating over transverse space, yields the nonrelativistic dispersion relation

$$D(\omega, k) = \epsilon_0^2 k^2 + \omega^2 - \frac{\omega^2}{\omega_{pe}^2} - i\Omega_0 + \omega_0^2 \left[1 - \frac{\omega^2}{\omega_{pe}^2} \right] \omega - \frac{\omega^2}{\omega_{pe}^2} + \omega_0^2 \quad (3)$$

where ω_b is the plasma frequency of the beam, Ω_0 the beam rotation for $(\omega - \omega_b - \omega_c)/2^{1/2}\omega_{pe}$, and ω_0 for $(\omega - \omega_c)^{1/2}\omega_{pe}$, and the mean-square transverse speed of the beam electrons, ω_{\perp}^2 , is defined by

$$\langle v_{\perp}^2 \rangle = 2\pi \int_0^\infty v_{\perp}^2 f(v_{\perp}) v_{\perp} dv_{\perp} \quad (4)$$

The function $Z(\Omega)$ is defined by

$$\left\{ \begin{array}{l} \int_0^{\infty} \frac{e^{-xt}}{t} \frac{d}{dt} \left(\frac{1}{t} \right) dt \\ \int_0^{\infty} \frac{e^{-xt}}{t} \frac{d}{dt} \left(\frac{1}{t} \right) dt = - \int_0^{\infty} e^{-xt} dt = - \frac{1}{x} \\ \int_0^{\infty} e^{-xt} dt = \frac{1}{x} \end{array} \right. \quad C_1 < 0$$

(3)

Since the function $\frac{1}{t}$ is decreasing, we have $\frac{d}{dt} \left(\frac{1}{t} \right) < 0$. Therefore, we can conclude that the integral $\int_0^{\infty} \frac{e^{-xt}}{t} \frac{d}{dt} \left(\frac{1}{t} \right) dt$ is converges. This is because the function e^{-xt} is decreasing and the function $\frac{d}{dt} \left(\frac{1}{t} \right)$ is also decreasing. Since the integral $\int_0^{\infty} \frac{e^{-xt}}{t} \frac{d}{dt} \left(\frac{1}{t} \right) dt$ is converges, we can conclude that the integral $\int_0^{\infty} e^{-xt} dt$ is also converges.

$\int_0^{\infty} e^{-xt} dt = \lim_{t \rightarrow \infty} \int_0^t e^{-xs} ds$

(3)

3. NUMERICAL SOLUTIONS OF THE DISPERSION RELATION

Whistler stability can be determined by solving the dispersion relation for ω complex and k real. In particular, wave growth occurs if the imaginary part, $\omega_i(k) < 0$. In this section, we shall examine some special cases. The type of instability concerned will be characterized in Section 4.

3.1 Zero Plasma and Beam Temperatures.

As $v_t, v_{t\parallel} \rightarrow 0$, Eq. (4) reduces to a form first derived by Bell and Buncman,⁶

$$D(\omega, k) = c^2 k^2 - \omega^2 + \frac{v_p^2 \omega}{\omega - \omega_c} + \omega_b^2 \left[\frac{\omega - kv_{0\parallel}}{\omega - \omega_c - kv_{0\parallel}} + \frac{k^2 \langle v^2 \rangle_1}{2(\omega - \omega_c - kv_{0\parallel})^2} \right] = 0 . \quad (8)$$

These authors analyzed Eq. (8) in the weak beam limit [$(\omega_b/\omega_c) \rightarrow 0$] with $\omega - kv_{0\parallel} \approx \omega_c$. This implies that the gyrating beam electrons 'see' the whistler frequency, ω , Doppler-shifted up to cyclotron resonance at ω_c , and may excite instability. As our numerical results will show, unstable waves are excited with essentially constant growth rate, over a very broad spectrum of frequency.

The way in which the interaction occurs is illustrated in Fig. 1. Figure 1(a) shows the uncoupled whistler, and the line along which the Doppler-shifted frequency ($\omega - kv_{0\parallel}$) equals ω_c . Since $\omega < \omega_c$, it should be noted that $v_{0\parallel} < 0$, i.e., the beam is directed opposite to the direction of propagation of the wave. Figure 1(b) illustrates the coupled modes in the absence of beam transverse energy. As $k \rightarrow \infty$ the upper branch approaches ω_c while the lower approaches the beam line. Note particularly that ω is real for all k real. This implies that no instability is excited, and agrees with the conclusion of Neufeld and Wright¹ for these conditions. Figure 1(c) illustrates the effect of beam transverse energy. There exists a value of k below which ω is real, and above which ω is complex. As $k \rightarrow \infty$, $\omega (\equiv \omega_r + i\omega_i)$

tends to

$$\omega_r = \omega_c + kv_{0\parallel}, \quad \omega_i = -\omega_b \left(\frac{\langle v_\perp^2 \rangle}{2c} \right)^{1/2}. \quad (9)$$

If k is real, there must be a pair of conjugate complex roots. The branch with $\omega_i > 0$ corresponds to decay, and is of no interest.

For the parameters of Fig. 1, the maximum growth rate is $(\omega_i/\omega_c) \approx 0.019$ corresponding to a temporal growth rate of 1.1 dB/cyclotron period. The corresponding ω_r and k are in the vicinity of the intersection of the two modes shown in Fig. 1(a). Physically, it might be expected that the most unstable waves would occur near that intersection since it is there that the gyrating beam electrons see the whistler propagating in the background plasma Doppler-shifted up to ω_c . On the other hand, the gain is only slightly lower well away from the coupling region, where the background plasma plays no role. This instability of the beam alone has been studied in detail by Bers, et al.⁸, using full relativistic theory.

3.2 Nonzero Plasma Temperature. Zero Beam Temperature.

For the case of $v_{t\parallel} = 0$, Eq. (4) reduces to

$$D(\omega, k) \equiv c^2 k^2 - \omega^2 - \frac{\omega_p^2 \omega}{2^{1/2} k v_t} Z(\xi_0) + \omega_b^2 \left[\frac{\omega - kv_{0\parallel}}{\omega - \omega_c - kv_{0\parallel}} + \frac{k^2 \langle v_\perp^2 \rangle}{2(\omega - \omega_c - kv_{0\parallel})^2} \right] = 0. \quad (10)$$

Figure 2 shows the effect of nonzero electron temperature on the unstable mode of Fig. 1(c). Even for $(v_t/c) = 0.02$, corresponding to a temperature of 102 eV, there is virtually no effect on the growth rate. Further computations show that even for $(v_t/c) = 0.05$, the maximum growth rate

is reduced by less than 10 percent below its value for $v_t = 0$. The implication is that in considering the instability, the plasma temperature can generally be ignored.

The physical reason for this can be made apparent by considering an alternative electron velocity distribution which happens to give a simple algebraic dispersion relation. Consider the resonance distribution,

$$f_p(v_{\parallel}, v_{\perp}) = \frac{(a/\pi^2)}{(v_{\parallel}^2 + v_{\perp}^2 + a^2)^2} . \quad (11)$$

We then obtain an expression similar to Eq. (8) but with $(\omega - \omega_c)$ in the plasma term replaced by $(\omega - \omega_c - ika)$.¹⁴ It is clear that thermal effects can be ignored if $|\omega - \omega_c| \gg |ka|$, i.e., if the intersection point between the beam line and the whistler dispersion curve is below the region where the whistler alone would be strongly cyclotron damped.

It is interesting to note that by the nature of the modification made to the dispersion relation for the case of a resonance distribution, there are no solutions with ω and k real simultaneously. We may easily demonstrate that this is also true for the Maxwellian. In Eq. (10), assume ω and k real, and set the real and imaginary parts equal zero. With use of Eq. (6), this yields

$$0 = \frac{\omega_p^2 \omega}{2^{1/2} k v_t} \exp \left[- \left(\frac{\omega - \omega_c}{2^{1/2} k v_t} \right)^2 \right] . \quad (12)$$

For ω_p , ω , v_t and k finite and nonzero, Eq. (12) cannot be satisfied. This is an important result. It implies that each mode of propagation is composed of waves that either all grow, or all decay, in time. Hence, if for some value of v_t it can be established that a mode has growing waves, then we can conclude that every wave in that mode must grow with time, and that this cannot be changed by varying the temperature of the background plasma.

3.3 Zero Plasma Temperature. Nonzero Beam Temperature.

We may consider two cases here separately. First is that of a spread in the beam transverse energy alone. It is clear from Eq. (4) that the details of this are unimportant, since only $\langle v_{\perp}^2 \rangle$ appears. Physically, this is simply a statement that all of the beam electrons see the same Doppler-shifted frequency $(\omega - kv_{0\parallel})$, which depends only on $v_{0\parallel}$, and can give up their transverse energy to the cyclotron resonance. This is not so for the second case: that of a spread in $v_{0\parallel}$. Under these conditions, and with $v_t = 0$, we have as the appropriate limiting form of Eq. (4),

$$D(\omega, k) \equiv c^2 k^2 - \omega^2 + \frac{\omega_p \omega}{\omega - \omega_c} + \omega_b^2 \left[1 - \frac{\omega_c}{2^{1/2} kv_{t\parallel}} Z(\xi) + \frac{\langle v_{\perp}^2 \rangle}{4v_{t\parallel}^2} Z'(\xi) \right] = 0 . \quad (13)$$

Figure 3 shows the dispersion characteristics of the unstable mode as $v_{t\parallel}$ varies. It will be seen that the growth rate is very sensitive to this quantity. The instability is essentially quenched when $(v_{t\parallel}/c) = 0.0045$, which corresponds to a temperature of only 5.2 eV compared with the beam energy of 640 eV.

It will be observed from Fig. 3 that there is a value of k , for any given $(v_{t\parallel}/c)$, above which the wave is damped. This value can be estimated as follows. Assume ω and k real, substitute from Eq. (6) in Eq. (13), and then separate real and imaginary parts. This yields,

$$\omega - kv_{0\parallel} + \left(\frac{1-\gamma}{\gamma} \right) \omega_c = 0 , \quad k^2 c^2 - \omega^2 + \frac{\omega_p \omega}{\omega - \omega_c} + (1-\gamma) \omega_b^2 = 0 , \quad (14)$$

where $\gamma = (\langle v_{\perp}^2 \rangle / 2v_{t\parallel}^2)$, and Eq. (7) has been used. Equation (14) is only cubic in k , and can easily be solved to determine the critical value at which $\omega_i = 0$.

4. INSTABILITY CLASSIFICATION

In Section 2, we have been considering waves propagating as $\exp i[\omega(k)t - kz]$ with k real and $\omega(k)$ satisfying the dispersion relation. For $\omega_1 < 0$ the plasma is unstable and, at first sight, no steady-state conditions appear possible. It was pointed out several years ago by Sturrock¹⁸ that there are actually two distinct types of instability. This distinction becomes apparent only after a spectrum of waves is superimposed by inversion of their Fourier and Laplace transforms. This inversion can be written in the form

$$A(z, t) = \int_C \frac{d\omega}{2\pi} \int \frac{dk}{2\pi} A(\omega, k) \exp i(\omega t - kz) , \quad (15)$$

where $A(\omega, k)$ is the spectral amplitude of the corresponding wave, and C is the Laplace contour in the lower half complex ω -plane, parallel to the real axis and below all singularities of the integrand.

As $t \rightarrow \infty$, Eq. (15) may describe one of the two forms shown in Fig. 4. The pulse disturbance may grow in time at every point in space, or it may propagate away while growing in time, eventually leaving the plasma at any given point quiescent. The former instability is termed "absolute", while the latter is termed "convective". The importance of making the distinction now becomes clear. If the instability is convective, it should be possible to excite propagating waves having real ω and complex k , i.e., growing in space away from the source. If the instability is absolute, there will be growth from noise until a saturation condition is reached everywhere, for which the small-signal theory breaks down.

This section will be devoted to a study of the whistler instabilities already introduced in Section II to determine their nature. To do so, we will use the now well-established method described by Derfler,¹³ and by Briggs,¹⁴ which consists of mapping the lower half of the complex ω -plane onto the complex k -plane by use of the dispersion relation. The stability criterion then states that an absolute instability is present

if a saddle-point is formed in the k -plane by the merging of two roots of the dispersion relation which come from opposite sides of the real axis. If, in the limit, as the imaginary part of ω tends to 0-, a root crosses the real k -axis without forming a saddle-point, the instability is said to be convective.

4.1 Zero Plasma and Beam Temperatures.

This procedure has been carried out for Eq. (8), and typical results are given in Fig. 5(a). It will be seen that, for the parameters chosen, a saddle-point is located at $(kc/\omega_c) = 7.29-i0.31$. The corresponding branch-point in the ω -plane is located at $(\omega_s/\omega_c) = 0.598-i0.062$. The growth rate of the absolute instability is given by $-(\omega_s)_i$ which corresponds to a gain of 3.4 dB/cyclotron period.

The locus of the branch-point is indicated in Fig. 6 as a function of the beam velocity and its transverse speed, and in Fig. 7(a) as a function of beam density (ω_b^2/ω_c^2) . Figure 7(b) shows the locus of the saddle-point in the k -plane as a function of beam density. These diagrams were obtained by solving numerically the simultaneous equations

$$D(\omega, k) = 0, \quad \frac{\partial D(\omega, k)}{\partial k} = 0, \quad (16)$$

where $D(\omega, k)$ is as given in Eq. (8). Note that the second part of Eq. (16) is equivalent to $(\partial u/\partial k) = 0$. Hence the roots of Eq. (16) are the positions of the saddle-points in the k -plane, and the corresponding branch-points in the ω -plane.

The curves in Fig. 6 show that, for a given $v_{0\parallel}$, the growth rate of the absolute instability can be lowered by decreasing $\langle v_\perp^2 \rangle^{1/2}$. On the other hand, for a given $\langle v_\perp^2 \rangle^{1/2}$, the growth rate tends to increase as $v_{0\parallel} \rightarrow 0$, reaches a maximum, and then approaches a non-zero limit for $v_{0\parallel} = 0$. Figure 7 shows that there is an optimum value of (ω_b^2/ω_c^2) , near 0.2, which maximizes $-\omega_i$, but that $-k_i$ increases with increasing (ω_b^2/ω_c^2) over the range examined.

We now wish to investigate conditions under which the absolute instability is quenched, to establish whether a convective instability persists. Two possible mechanisms for quenching the absolute instability

will be considered: collisions, and non-zero plasma electron temperature.

4.2 Effect of Collisions.

Electron-neutral momentum transfer collisions occurring with frequency ν can be accounted for by including a collision term in the Boltzmann equation for the plasma electrons. The only modification made to Eq. (8) is that $(\omega - \omega_c)$ in the plasma term changes to $(\omega - i\nu - \omega_c)$.

The locus of the branch-point as ν and $\langle v_{\perp}^2 \rangle^{1/2}$ vary is shown in Fig. 8(a). It will be seen that, for the parameters chosen, for $\langle v_{\perp}^2 \rangle^{1/2}/c = 0.025$, the branch-point crosses the real ω axis when $(\nu/\omega_c) = 0.033$. For higher collision frequencies, the absolute instability is not present since $(\omega_s)_i > 0$. There is, however, a convective instability, as the k-plane plot of Fig. 5(b) for this case indicates. For the remaining two values of $\langle v_{\perp}^2 \rangle^{1/2}/c$ in Fig. 8(a), very high collision frequencies would be required to stabilize the absolute instability.

It is interesting to examine how collisions modify the dispersion characteristics. Figure 8(b) illustrates this for the parameters of Fig. 5(b). There is a weak maximum in k_i , near the coupling point between the beam line and the plasma mode, corresponding to a growth rate of a few dB/wavelength.

4.3 Effect of Plasma Temperature.

This may be understood most simply by choosing for the plasma electron velocity distribution a judicious approximation to the Maxwellian. We shall again assume the resonance distribution of Eq. (11), so that the dispersion relation is given by Eq. (8) with the denominator of the plasma term changed from $(\nu - \omega_c)$ to $(\omega - ika - \omega_c)$. The treatment is then similar to that for collisions.

By making (a/c) sufficiently large, the absolute instability can be eliminated, and a convective instability can be uncovered. For example, for the parameters of Fig. 8 and $\langle v_{\perp}^2 \rangle^{1/2}/c = 0.025$, the critical thermal velocity to quench the absolute instability is given

is given by $(a/c) = 0.0045$. The spatial growth rates are then comparable to those indicated in Fig. 8(b).

Computations for the Maxwellian distribution have been made using Eq. (10). The results are shown in Fig. 9. They illustrate that temperatures above 100 eV are necessary to stabilize the absolute instability for $(\langle v_{\perp}^2 \rangle^{1/2}/c) \geq 0.025$. When the absolute instability is stabilized, a weak convective instability remains.

4.4 Effect of Beam Temperature.

It was pointed out in Section 3.3 that only a small longitudinal beam temperature is necessary to stabilize the absolute instability. Figure 10 has been computed from Eq. (13) and shows the branch-point locus for three beam transverse energies. The ratio $[v_{t\parallel}^2/\langle v_{\perp}^2 \rangle]$ required for stabilization is approximately 0.04 in all three cases. For thermal energies in excess of this, there is weak convective instability, as in the previous cases.

5. COMPETING INSTABILITIES

In addition to the whistler instability which may be excited by a gyrating electron beam, at least two longitudinal wave instabilities may be excited. The first is in the cyclotron harmonic wave (CHW) mode, and needs only a nonzero transverse component of beam energy. The second is a beam/plasma interaction parallel to the magnetic field, and needs only a longitudinal component of beam energy. In this section we shall consider the growth characteristics of these two modes.

5.1 Cyclotron Harmonic Waves ($k_{\parallel} = 0$).

These waves are described by the dispersion relation^{15,19}

$$1 + \sum_{\parallel} \frac{\omega_p^2}{k_{\parallel}^2 + k_{\perp}^2} \sum_{n=-\infty}^{\infty} \int_{-\infty}^{\infty} dv_{\parallel} \frac{H_n(v_{\parallel})}{\omega - k_{\parallel} v_{\parallel} - n\omega_c} = 0 \quad (\omega_1 < 0) ,$$

$$H_n(v_{\parallel}) = 2\pi \int_0^{\infty} dv_{\perp} \left(\frac{n\omega_c}{v_{\perp}} \frac{\partial f_0}{\partial v_{\perp}} + k_{\parallel} \frac{\partial f_0}{\partial v_{\parallel}} \right) J_n^2 \left(\frac{k_{\perp} v_{\perp}}{\omega_c} \right) v_{\perp} . \quad (17)$$

where k_{\perp} and k_{\parallel} ($= k$ in previous sections) are the components of the wave vector perpendicular and parallel to the magnetic field, respectively, and the first summation in Eq. (17) extends over all charged particle species present. For $k_{\perp} = 0$, Eq. (17) describes electrostatic wave propagation with no effects due to the static magnetic field. For $k_{\parallel} = 0$, we obtain

$$1 - \sum_{\parallel} \frac{\omega_p^2}{\omega_c^2} \sum_{n=-\infty}^{\infty} a_n(k_{\perp}) \frac{n\omega_c}{\omega - n\omega_c} = 0 , \quad a_n(k_{\perp}) = - \frac{\omega_c^2}{k_{\perp}^2} \int dv_{\perp} \frac{1}{v_{\perp}} \frac{\partial f_0}{\partial v_{\perp}} J_n^2 \left(\frac{k_{\perp} v_{\perp}}{\omega_c} \right) , \quad (18)$$

for which numerous solutions have been obtained. Here we shall consider two distributions: The Maxwellian, and the ring distribution given by

$$f_0(v_{\parallel}, v_{\perp}) = \delta(v_{\perp} - v_{0\perp}) \delta(v_{\parallel} - v_{0\parallel}) / 2\pi v_{0\perp} , \quad (\text{Ring}) . \quad (19)$$

For the Maxwellian, the dispersion relation is

$$1 - \frac{\omega_p^2}{\omega_c^2} \sum_{n=-\infty}^{\infty} \frac{\exp(-\lambda) I_n(\lambda)}{\lambda} \frac{n\omega_c}{\omega - n\omega_c} = 0 , \quad (20)$$

where λ has been written for $(k_{\perp} v_t / \omega_c)^2$, and I_n is a modified Bessel function of the first kind. Figure 11 shows the dispersion characteristics described by Eq. (20). For a specified value of $(\omega_p^2 / \omega_c^2)$, propagating branches lie between successive cyclotron harmonics, and there is a real ω solution for any real k_{\perp} , i.e. the distribution is stable. More generally, if $(\partial f_0 / \partial f_{\perp}) < 0$, for all $v_{\perp} > 0$, this is always true. The ring distribution is an example for which this is not satisfied. It has the dispersion relation,

$$1 - \frac{\omega_p^2}{\omega_c^2} \sum_{n=-\infty}^{\infty} \frac{dJ_n^2(\mu)}{d\mu} \frac{n\omega_c}{\omega - n\omega_c} = 0 , \quad \mu = \frac{k_{\perp} v_{0\perp}}{\omega_c} . \quad (21)$$

Figure 12 shows the numerical solution for $\omega(k_{\perp})$ for two values of $(\omega_p^2 / \omega_c^2)$. If this parameter is relative small, each propagating branch undulates about a harmonic of ω_c . As $(\omega_p^2 / \omega_c^2)$ increases, two successive branches can couple, leading to regions in the dispersion characteristics where the ω is complex for real k_{\perp} , and instability is present. The imaginary frequency components can become very strong indeed. For example, in Fig. 12 (ω_1 / ω_c) is of order unity, and growth rates of the order of 50 dB/cyclotron period are implied. This figure is to be compared with the more modest growth rates of about 1 dB/cyclotron period found for the whistler instability.

To compare electrostatic instabilities of perpendicularly propagating CHW, and the electromagnetic instabilities of the whistler mode, we shall consider a plasma containing a fraction, α , of the electrons in a Maxwellian distribution, and the remaining fraction $(1-\alpha)$ in a ring electron velocity distribution. This system has the dispersion relation,

$$1 - \frac{\omega_p^2}{\omega_c^2} \left[\alpha \sum_{n=-\infty}^{+\infty} \frac{\exp(-\lambda) I_n(\lambda)}{\lambda} \frac{n\omega_c}{\omega - n\omega_c} + (1-\alpha) \sum_{n=-\infty}^{\infty} \frac{1}{\mu} \frac{dJ_n^2(\mu)}{d\mu} \frac{n\omega_c}{\omega - n\omega_c} \right] = 0 \quad (22)$$

where we note that in this subsection only ω_p^2 refers to the total electron density ($\equiv (\omega_p^2 + \omega_b^2)$) elsewhere.

Figure 12 shows the threshold conditions for instability in the first four frequency bands obtained numerically from Eq. (22). When $\alpha = 0$, all electrons are in the ring group, instability first occurs in the passband $2\omega_c < \omega < 3\omega_c$ for $(\omega_p^2/\omega_c^2) = 6.62$. In the passbands $0 < \omega < \omega_c$, $\omega_c < \omega < 2\omega_c$ and $3\omega_c < \omega < 4\omega_c$, the threshold conditions for instability occur, respectively, at $(\omega_p^2/\omega_c^2) = 17.02$, 6.81, and 6.94. As α increases, the threshold conditions become strongly dependent on the velocity ratio (v_{01}/v_t) . Indeed, in some cases, the threshold condition may be lowered if (v_{01}/v_t) is sufficiently large. Figures 13(b) and 13(c) show that instability is predicted for values of (ω_p^2/ω_c^2) that correspond to stability when the electrons are exclusively in the ring group. This also has the effect of increasing the maximum attainable growth rate of the instability in a given frequency band. This is clearly illustrated in Fig. 14 where the maximum value of (ω_1/ω_c) is plotted as a function of α . It will be seen that the growth rate of instabilities associated with the ring distribution alone can be increased by adding to that distribution a group of Maxwellian electrons.

These results suggest that CHW instabilities might compete strongly with the whistler instability. The electrostatic instability will not dominate, however, when $\alpha \approx 1$, corresponding to a weak beam passing through a plasma. Figure 13 indicates that for $\alpha \approx 1$, it is only when $v_{01} \gg v_t$ that instability can be excited, and then only for a very narrow band of (ω_p^2/ω_c^2) . For the parameter values used in the whistler computations: $(\omega_p^2 + \omega_b^2)/\omega_c^2 = 26$, $\alpha = 0.96$, $(v_t/c) = 0.02$ and $(v_{01}/c) = 0.025$, we have $(v_{01}/v_t) = 1.25$, which is well within the stable region of the diagrams shown in Fig. 13. An additional factor is that the CHW growth depends strongly on $f(v_\perp)$, whereas the

whistler growth is incompatible to transverse beam energy spread. It appears safe to conclude that whistler wave beam instabilities are electromagnetic instabilities of perpendicular propagating CIV will generally be negligible compared to the whistler instabilities.

3.2 Longitudinal Beam Plasma Interaction (b) - 0)

For this case, Eq. (17) reduces to

$$1 - \sum_{s=1}^3 \frac{v_p^2}{k_\parallel^2} \int \frac{s v_{t\parallel}^2 v_s}{v_{t\parallel}^2 + (v_{t\parallel}^2 - k_\parallel^2)} \epsilon_s = 0 \quad (22)$$

where the summation is over all particle species. We assume that the plasma and beam electrons have velocity distributions of Eq. (2) and neglect ion motions. The dispersion relation becomes

$$1 - \frac{v_p^2}{2v_{t\parallel}^2 k_\parallel^2} Z(\epsilon_0) - \frac{v_b^2}{2v_{t\parallel}^2 k_\parallel^2} Z(\epsilon) = 0 \quad (23)$$

where ϵ_0 and ϵ are now $(\omega/2)^{1/2} k_\parallel v_{t\parallel}$ and $((\omega - k_\parallel v_{t\parallel})^2/4 - \omega^2/k_\parallel^2)^{1/2} k_\parallel v_{t\parallel}$.

Consider first the case where the background plasma is cold ($v_t = 0$). Equation (24) then reduces to

$$1 - \frac{v_p^2}{2} \cdot \frac{v_b^2}{v_{t\parallel}^2 k_\parallel^2} [1 + \epsilon Z(\epsilon)] = 0 \quad (24)$$

To determine conditions for marginal stability, assume ϵ and k_\parallel real, and set the real and imaginary parts of Eq. (24) equal to zero. This yields

$$1 - \frac{\omega_p^2}{\omega^2} + \frac{\omega_b^2}{v_{t\parallel}^2 k_\parallel^2} \left\{ 1 + \epsilon [Z(\epsilon)]_r \right\} = 0 \quad , \quad \frac{v_b^2}{v_{t\parallel}^2 k_\parallel^2} \epsilon [Z(\epsilon)]_i = 0 \quad (25)$$

It is readily established that $\omega_i \neq 0$ if ω and k_{\parallel} are finite and nonzero. Hence, we conclude from Eq. (26) that

$$\omega - k_{\parallel} v_{0\parallel} = 0, \quad 1 - \frac{\omega_p^2}{\omega^2} + \frac{\omega_b^2}{v_{t\parallel}^2 k_{\parallel}^2} = 0. \quad (27)$$

Equation (27) determines k_{\parallel} at which ω is just real. We have

$$k_{\parallel}^2 = \frac{\omega_p^2}{v_{0\parallel}^2} - \frac{\omega_b^2}{v_{t\parallel}^2}. \quad (28)$$

From Eq. (26) we see that if $|v_{t\parallel}| < (\omega_b/\omega_p)|v_{0\parallel}|$, $k_{\parallel}^2 < 0$, implying that the critical wave-number is purely imaginary. This violates our initial assumption that both k_{\parallel} and ω are real. Hence, when this inequality is satisfied, all waves with $k_{\parallel} > 0$ must have ω complex. We know that if $v_{t\parallel} = 0$, then there exists one mode of propagation which has growing waves.¹⁴ If $v_{t\parallel} > 0$, but within the limits specified by the inequality, every wave belonging to that mode will have a complex frequency with $\omega_i < 0$, and will grow with time. The situation changes if $|v_{t\parallel}| > (\omega_b/\omega_p)|v_{0\parallel}|$, since now $k_{\parallel}^2 > 0$, as defined by Eq. (27). Hence, there is one positive value of k_{\parallel} at which ω is real.

When the results obtained here are compared with the instability threshold conditions of the whistler mode in the same beam/plasma model, there appears to be almost an inverse relationship between the two cases. For example, when the beam velocity has a thermal spread and the background plasma is cold, waves with large k_{\parallel} are heavily damped by a relatively small beam temperature. Only waves with small k_{\parallel} can grow in time, but the growth rate is almost zero. For the electrostatic waves, it appears that waves with small k_{\parallel} are the first to be damped, but only if the thermal speed of the beam electrons exceeds a critical

number defined by $|v_{c\parallel}| = (v_b/v_p) |v_{0\parallel}|$. For smaller thermal speeds, all waves in the mode grow with time. In the whistler instability studies, we used $(\omega_p^2/\omega_c^2) = 25$, $(v_b^2/\omega_c^2) = 1$, and $(v_{0\parallel}/c) = -0.05$. With these values we obtain $|v_{c\parallel}| = 0.01c$, which exceeds the thermal speed of $0.004c$ that was found to be needed to reduce the growth rate of the whistler instability very significantly.

Finally, we consider the case where the background plasma is hot and the parallel beam temperature is zero. The dispersion relation for this case is

$$1 + \frac{\omega_p^2}{v_t^2 k_\parallel^2} \left[1 + \frac{\omega}{2^{1/2} v_t k_\parallel} Z\left(\frac{\omega}{2^{1/2} v_t k_\parallel}\right) \right] - \frac{\omega_b^2}{(\omega - v_{0\parallel} k_\parallel)^2} = 0. \quad (29)$$

Assuming ω and k_\parallel real, and setting the real and imaginary parts of Eq. (29) equal to zero, yields

$$\begin{aligned} 1 + \frac{\omega_p^2}{v_t^2 k_\parallel^2} \left\{ 1 + \frac{\omega}{2^{1/2} v_t k_\parallel} \left[Z\left(\frac{\omega}{2^{1/2} v_t k_\parallel}\right) \right]_R \right\} - \frac{\omega_b^2}{(\omega - v_{0\parallel} k_\parallel)^2} &= 0 \\ \frac{\omega_p^2}{v_t^2 k_\parallel^2} \left(\frac{\omega}{2^{1/2} v_t k_\parallel} \right) \left[Z\left(\frac{\omega}{2^{1/2} v_t k_\parallel}\right) \right]_I &= 0 \end{aligned} \quad (30)$$

Since $Z_I \neq 0$ if ω is non-zero and k_\parallel is finite, Eq. (29) cannot be satisfied. Hence, there are no solutions of Eq. (29) where both ω and k_\parallel are real. The implication of this result is that the instability cannot be quenched simply by increasing the electron temperature in the background plasma. It will be recalled from Section 3.2 that the whistler instability also has this property.

If the plasma temperature tends to zero, Eq. (30) reduces to the usual cold beam/plasma interaction expression which predicts an infinite

convective growth rate at the plasma frequency.¹⁴ Provided the beam velocity exceeds the plasma thermal velocity by an order of magnitude, Eq. (30) will predict growth rates typically of many tens of dB/wavelength for the parameters used in our whistler calculations.^{20,21}

To demonstrate this, we replace Eq. (29) by the approximate expression

$$1 - \frac{\omega_p^2}{\omega^2 - 3k_{\parallel}^2 v_t^2} - \frac{\omega_b^2}{(\omega - v_{0\parallel} k_{\parallel})^2} = 0, \quad (31)$$

solutions for which have been given elsewhere.²¹ Equation (31) may be solved for $(k_{\parallel 1}/k_{\parallel r})$ small to give

$$\frac{k_{\parallel r} c}{\omega_c} \approx \frac{(\omega_p/\omega_c)}{(v_{0\parallel}/c)}, \quad \frac{k_{\parallel 1} c}{\omega_c} \approx 0.44 \frac{(\omega_p/\omega_c)}{(v_{0\parallel}/c)} \left(\frac{\omega_b^2}{\omega_p^2} \right)^{1/3} \left(\frac{v_{0\parallel}}{v_t} \right)^{2/3}, \quad (32)$$

as the conditions for maximum growth. For our usual parameters, Eq. (32) gives $(k_{\parallel r} c/\omega_c) \approx 100$, $(k_{\parallel 1} c/\omega_c) \approx 15 (v_{0\parallel}/v_t)^{2/3}$. The growth rate is enormously greater than for the convective whistler instabilities (see for example Figs. 7(b), and 8(b)). It may be argued that since this maximum growth occurs for $\omega \approx \omega_p$, the growth should actually be computed for $(\omega/\omega_c) < 1$ for a strict comparison. This is not so, since the beam/plasma growth will certainly dominate the situation, and ultimately spread the beam velocity. This makes the validity of the whistler computations somewhat hypothetical.

6. DISCUSSION

The computations presented in Sections 3 and 4 indicate that gyrating electron beams can excite weakly growing absolute instabilities in the whistler mode. These can be quenched by high collision frequencies or electron temperature in the background plasma, or by a small longitudinal beam temperature. A weak convective instability remains. Section 5 indicates that, for the same parameters, strong longitudinal beam/plasma interaction can be obtained, but growth in perpendicularly propagating CHW is probably negligible. We may now consider these results in relation to laboratory and space plasmas. First, as far as fusion study machines with beam injection are concerned, it seems likely that the longitudinal wave instabilities will be most important. It should also be remarked that a more common instability in such applications is probably that appropriate to the loss-cone electron velocity distribution. This distribution is formed through loss of particles from the ends of magnetic mirror machines. It is also subject to longitudinal wave instabilities.²² From the point of view of devices, it is strongly implied that whistler amplification is too weak for use in microwave beam/plasma amplifiers competitive with currently available devices.

Finally, we consider the magnetosphere, for which whistler growth mechanisms have long been postulated to explain phenomena such as VLF emissions, and very long multiple-hop whistler trains.^{23,24} In such special regions as the bow shock, where a stream of charged particles impinges on the earth's magnetic field, there may well be a gyrating beam type distribution. Elsewhere, the distribution is more likely that of a high energy loss-cone distribution interacting with a dense background of effectively cold plasma.^{9,12} This specific distribution requires more intensive study than it has received so far to cover the two important points emphasized in our treatment here: determination of the nature of the instability, and comparison with competing instabilities.

Several general points may be made in amplification of these last comments. The first covers the nature of the instability. To maintain the amplitude of whistlers in very long whistler trains, some type of convective instability suggests itself, the constant amplitude observed representing a saturation effect. It would be very useful, then,

to establish whether the loss-cone distribution combined with a cold background plasma leads to convective growth in both directions along the magnetic field lines, rather than to absolute instability. Absolute instability is more likely to give rise to continuous VLF emissions of the hiss type.

The existence of competing longitudinal wave instabilities raises an interesting point concerning whistler amplification observed from the ground. The growth may not be in the whistler mode itself, but in some other mode to which the whistler couples at entry and exit from the active region. This point does not seem to have received attention in the whistler literature. A second point concerning competing instabilities is that our comparisons are of growth rates based on small-signal dispersion relations. It is also important to establish the saturation levels, which can be reached by the various modes, and this can only be determined from nonlinear theory. It is possible that a slower growing whistler mode might ultimately reach a higher amplitude than a rapidly growing longitudinal instability. For the beam-type distribution, it is very likely that the beam/plasma interaction along the magnetic field lines will dominate, since many experiments have shown that this type of interaction can grow to amplitudes sufficient to disperse the beam completely, whereas Section 4.3 indicated that only a small beam velocity spread would quench the whistler instability. It has been suggested in the literature⁶ that conditions are accessible in which the small-signal whistler growth would be the stronger. Whether this is so, and whether the large-signal amplitudes would continue this trend, are still open questions.

ACKNOWLEDGEMENTS

This work was supported by the National Aeronautics and Space Administration, and by the Advanced Projects Research Agency, Department of Defense, as part of PROJECT DEFENDER.

REFERENCES

1. J. Neufeld and H. Wright, Phys. Rev. 129 (1963) 1489.
2. D. B. Chang, Astrophys. J., 138 (1963) 1231.
3. R. N. Sudan, Phys. Fluids 6 (1963) 57.
4. R. N. Sudan, Phys. Fluids 8 (1965) 153.
5. R. N. Sudan, Phys. Rev. 139 (1965) A78.
6. T. F. Bell and O. Buneman, Phys. Rev. 133 (1964) A 1300.
7. H. Guthart, J. Res. NBS 69D (1965) 1403.
8. A. Bers, J. K. Hoag, and E. A. Robertson, MIT Research Laboratory of Electronics, QSR 77 (1965) 149; 78, 105; 79, 107.
9. H. B. Liemohn, J. Geophys. Res. 72 (1967) 39.
10. J. E. Scharer and A. W. Trivelpiece, Phys. Fluids 10 (1967) 591.
11. J. E. Scharer, Phys. Fluids 10 (1967) 652.
12. A. C. Das, J. Plasma Phys. 1 (1967) 29.
13. H. Derfler, Proc. Vth International Conference on Ionization Phenomena in Gases, Munich, Germany, August 1961 (North-Holland Pub. Co., 1962) p. 1423.
14. R. J. Briggs, Electron Stream Interaction with Plasmas (MIT Press, Cambridge, Mass. 1964).
15. T. H. Stix, The Theory of Plasma Waves (McGraw-Hill Book Company, New York, 1962).
16. D. C. Montgomery and D. A. Tidman, Plasma Kinetic Theory (McGraw-Hill Book Company, New York, 1964).
17. B. D. Fried and S. D. Conte, The Plasma Dispersion Function (Academic Press, New York, 1961).
18. P. A. Sturrock, Phys. Rev. 112 (1958) 1488.
19. I. B. Bernstein, Phys. Rev. 109 (1958) 10.

20. E. E. Abraham and F. W. Crawford, Proc. VIIth International Conference on Phenomena in Ionized Gases, Belgrade, Yugoslavia, August 1965
(Gradevinska Knjiga Pub. House, Belgrade 1966) Vol. 2, 377.
21. F. W. Crawford, Int. J. Elect. 19 (1965) 217.
22. R. F. Post and M. N. Rosenbluth, Phys. Fluids 9 (1966) 730.
23. R. A. Helliwell, Whistlers and Related Ionospheric Phenomena,
(Stanford University Press, Stanford, California, 1965).
24. R. A. Helliwell, J. Geophys. Res. 72 (1967) 4773.

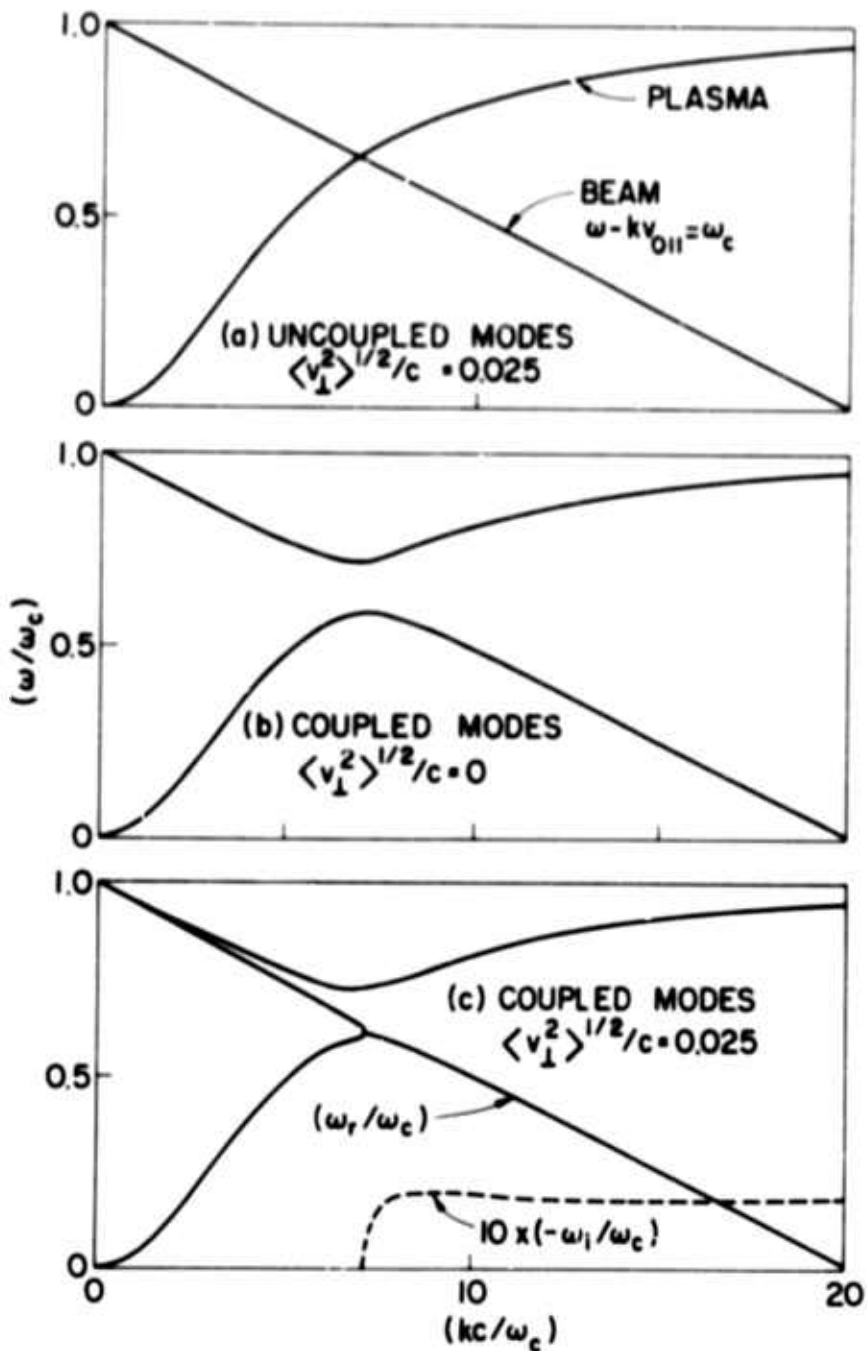


FIG. 1. WHISTLER INSTABILITIES: MODE COUPLING FOR ZERO PLASMA AND BEAM TEMPERATURES

$$[(v_p^2/\omega_c^2) = 25, (\omega_b^2/\omega_c^2) = 1, (v_{0\parallel}/c) = -0.05]$$

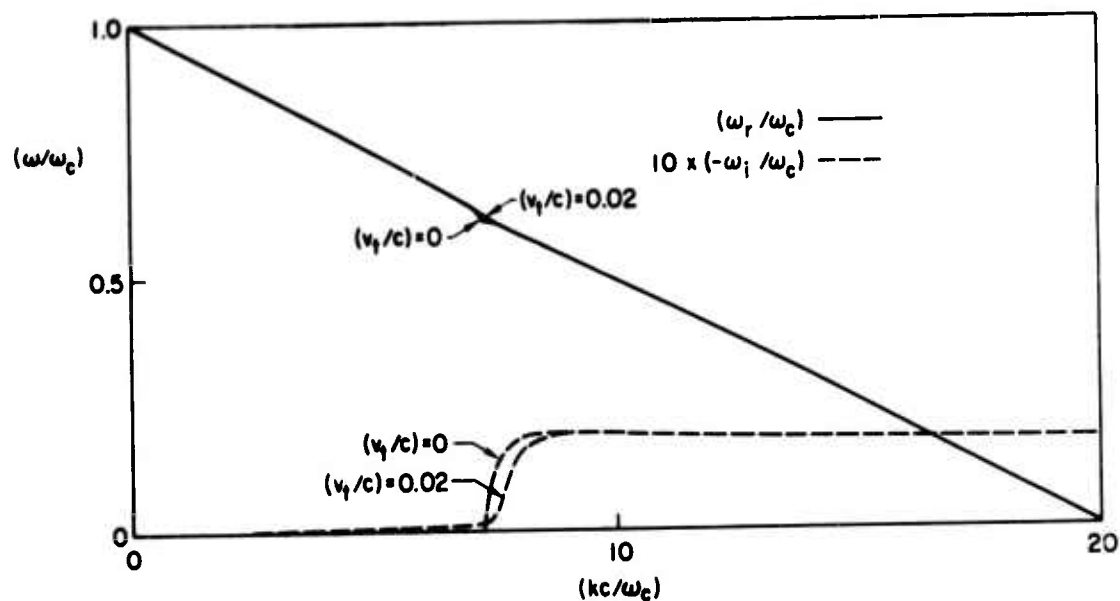


FIG. 2. EFFECT OF NONZERO PLASMA TEMPERATURE ON THE UNSTABLE MODE OF FIG. 1(c) [$(\omega_p^2/\omega_c^2) = 25$, $(\omega_b^2/\omega_c^2) = 1$, $(v_{0\parallel}/c) = -0.05$, $(\langle v_\perp^2 \rangle^{1/2}/c) = 0.025$].

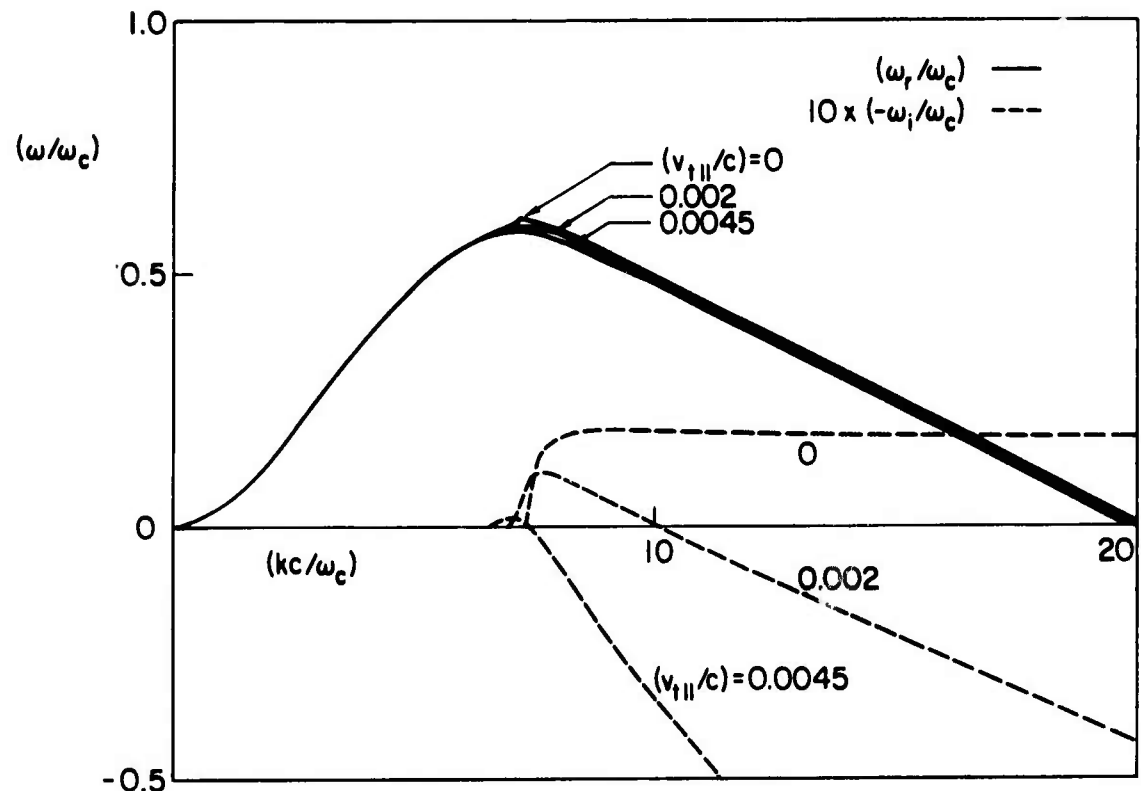


FIG. 3. EFFECT OF NONZERO BEAM TEMPERATURE ON THE UNSTABLE MODE OF FIG. 1(c) [$(\omega_p^2/\omega_c^2) = 25$, $(\omega_b^2/\omega_c^2) = 1$, $(v_{0\parallel}/c) = -0.05$, $(\langle v_\perp^2 \rangle^{1/2}/c) = 0.025$].

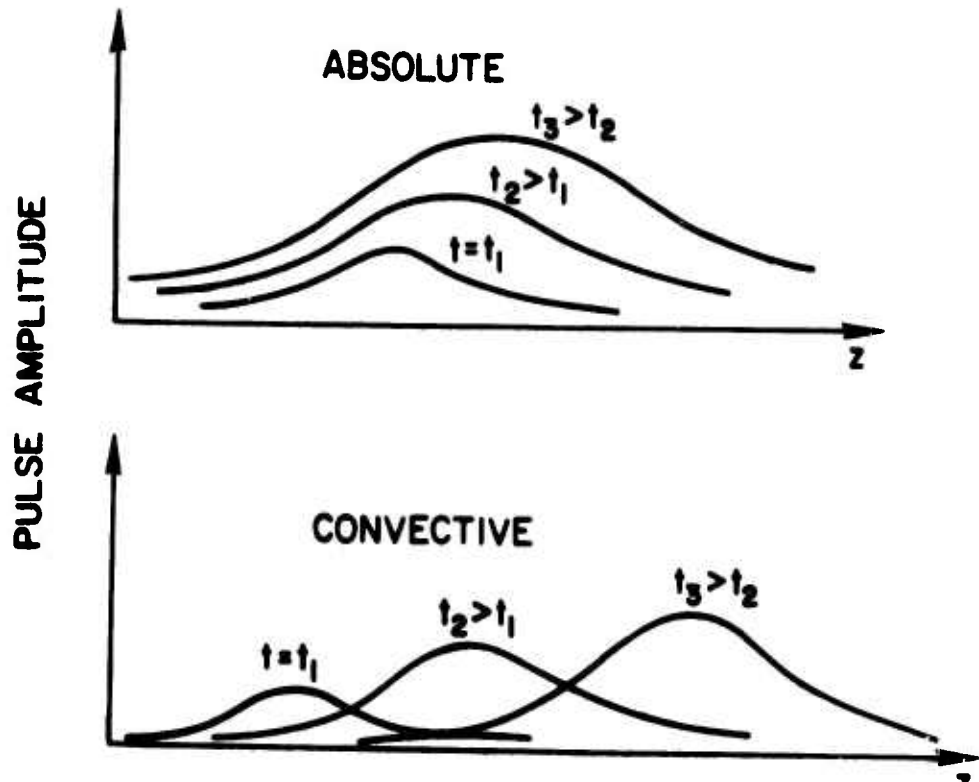


FIG. 4. ABSOLUTE AND CONVECTIVE INSTABILITIES.

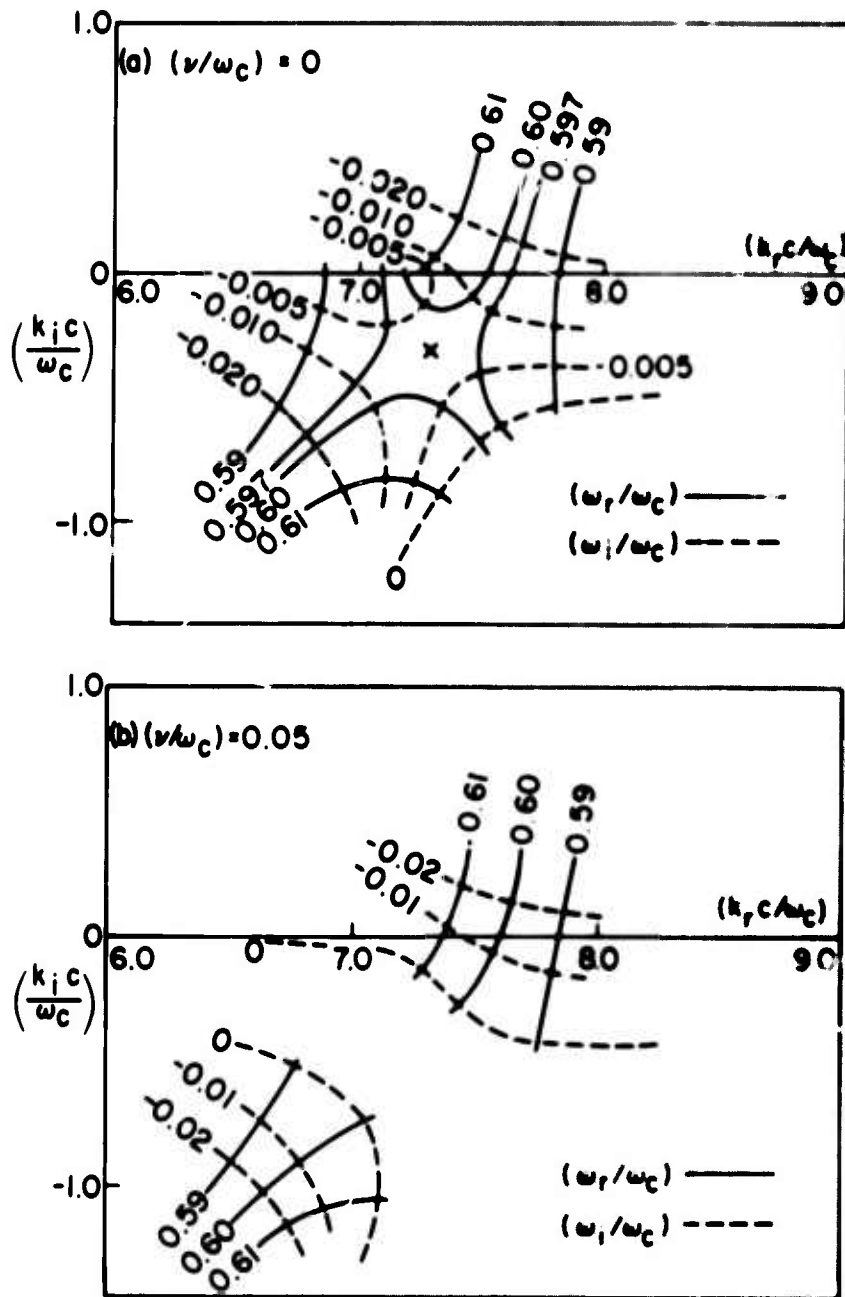


FIG. 5. STABILITY ANALYSIS: k -PLANE PLOT

$$[(\omega_p^2/\omega_c^2) = \omega_b, (\omega_b/\omega_c) = 1, (\langle v_\perp \rangle^{1/2}/c) = 0.5, \\ (\nu_0/\omega_c) = 0.05].$$

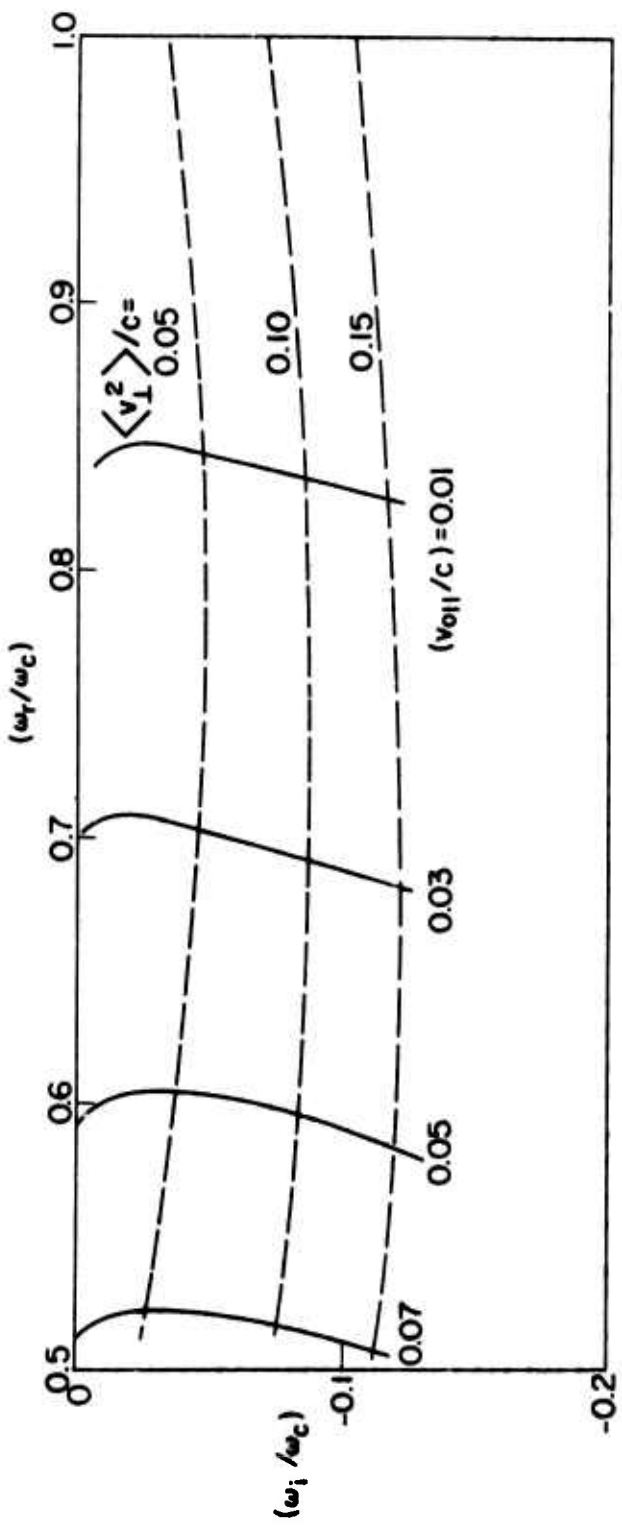


FIG. 6. STABILITY ANALYSIS: LOCI OF BRANCH-POINTS IN THE COMPLEX ω -PLANE
 $[(\omega_p^2/\omega_c^2) = 25, (\omega_b^2/\omega_c^2) = 1]$.

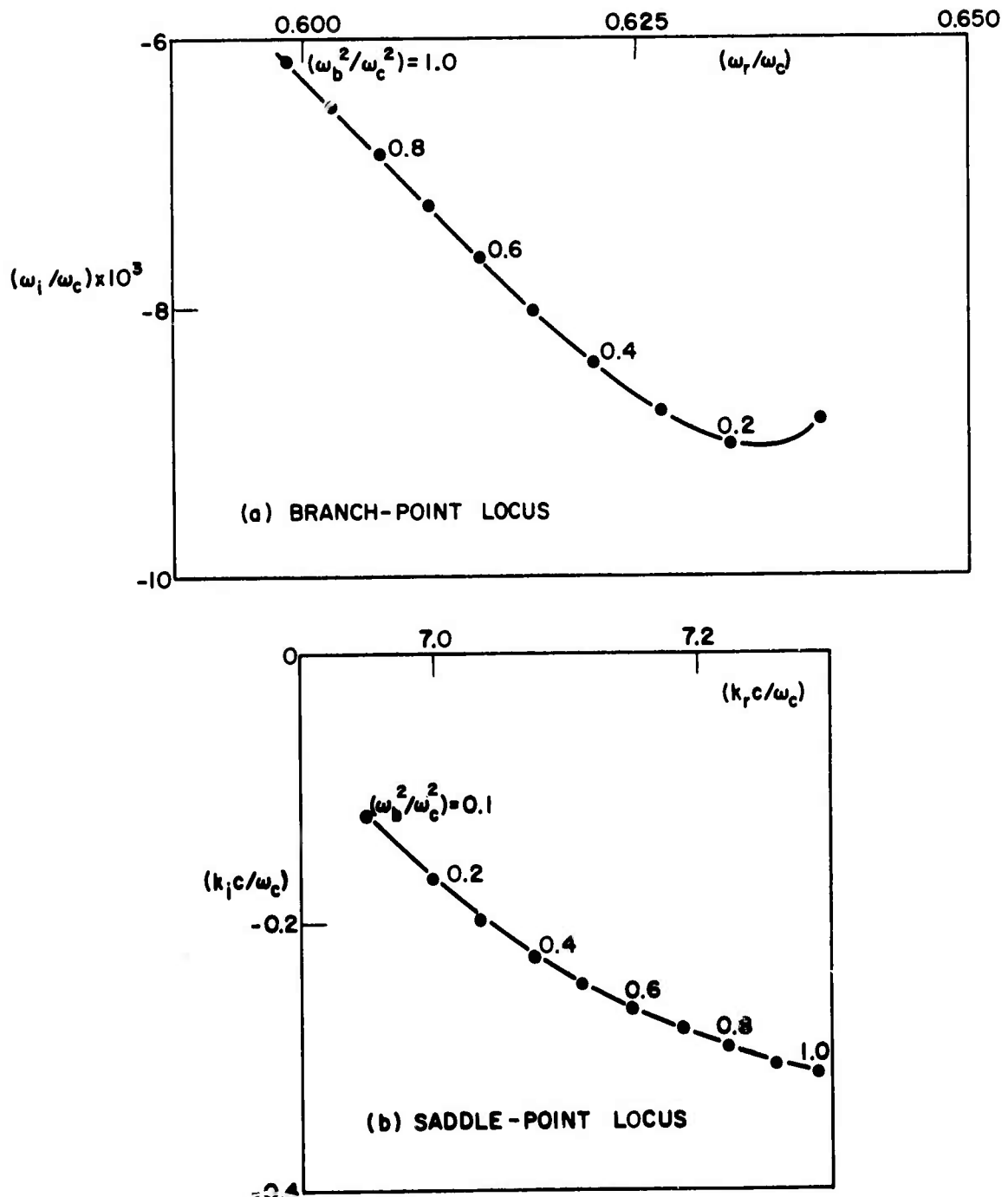


FIG. 7. STABILITY ANALYSIS: LOCI OF BRANCH-POINTS IN THE ω -PLANE AND SADDLE-POINTS IN THE k -PLANE, WITH VARYING (ω_b^2/ω_c^2) [$(\omega_p^2/\omega_c^2) = 25$, $(v_{0\parallel}/c) = -0.05$, $(\langle v_\perp^2 \rangle^{1/2}/c) = 0.025$].

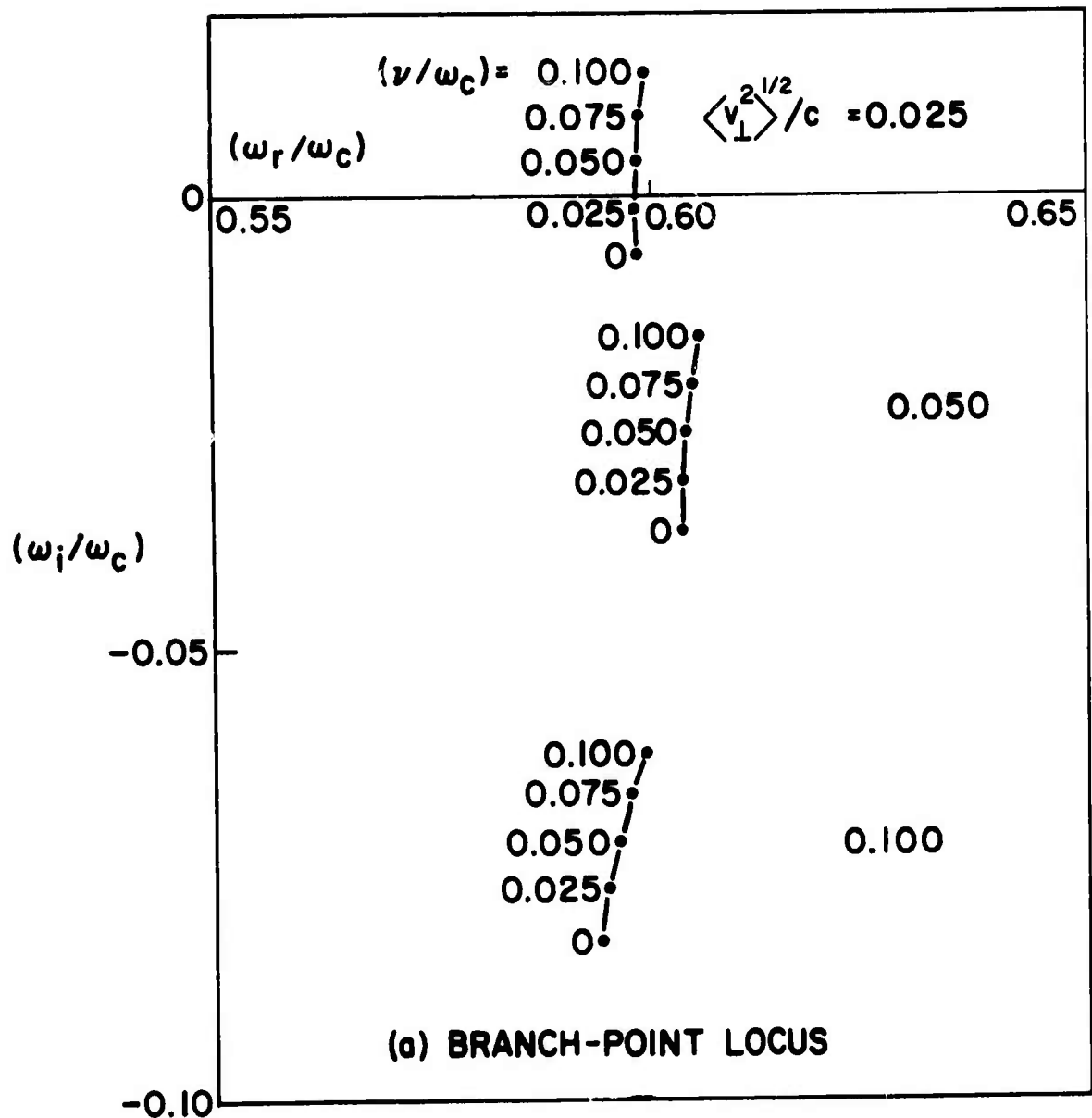


FIG. 8(a). STABILITY ANALYSIS: EFFECT OF COLLISIONS
 $[(\omega_p^2/\omega_c^2) = 25, (\omega_b^2/\omega_c^2) = 1]$.

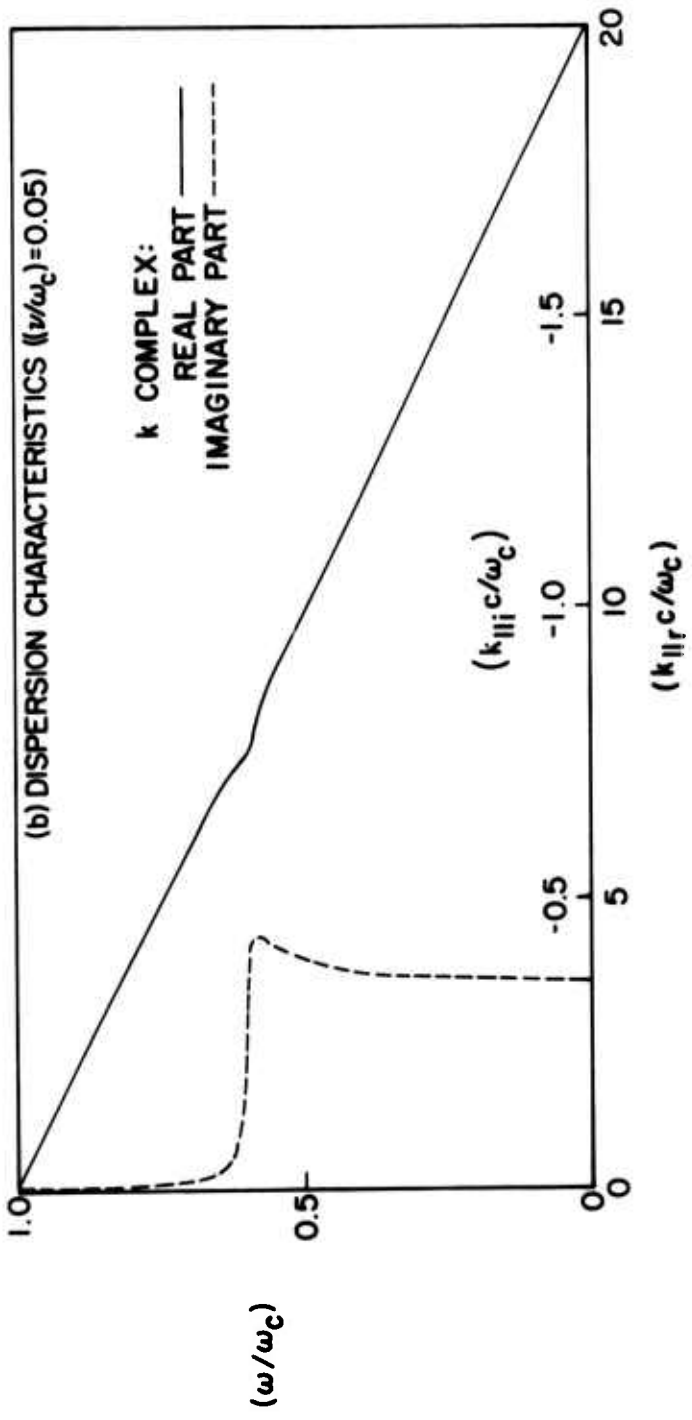


FIG. 8 (b). STABILITY ANALYSIS: EFFECT OF COLLISIONS
 $[(\omega_p^2/\omega_c^2) = 25, (\omega_b^2/\omega_c^2) = 1, (v_0 \parallel/c) = -0.05]$.

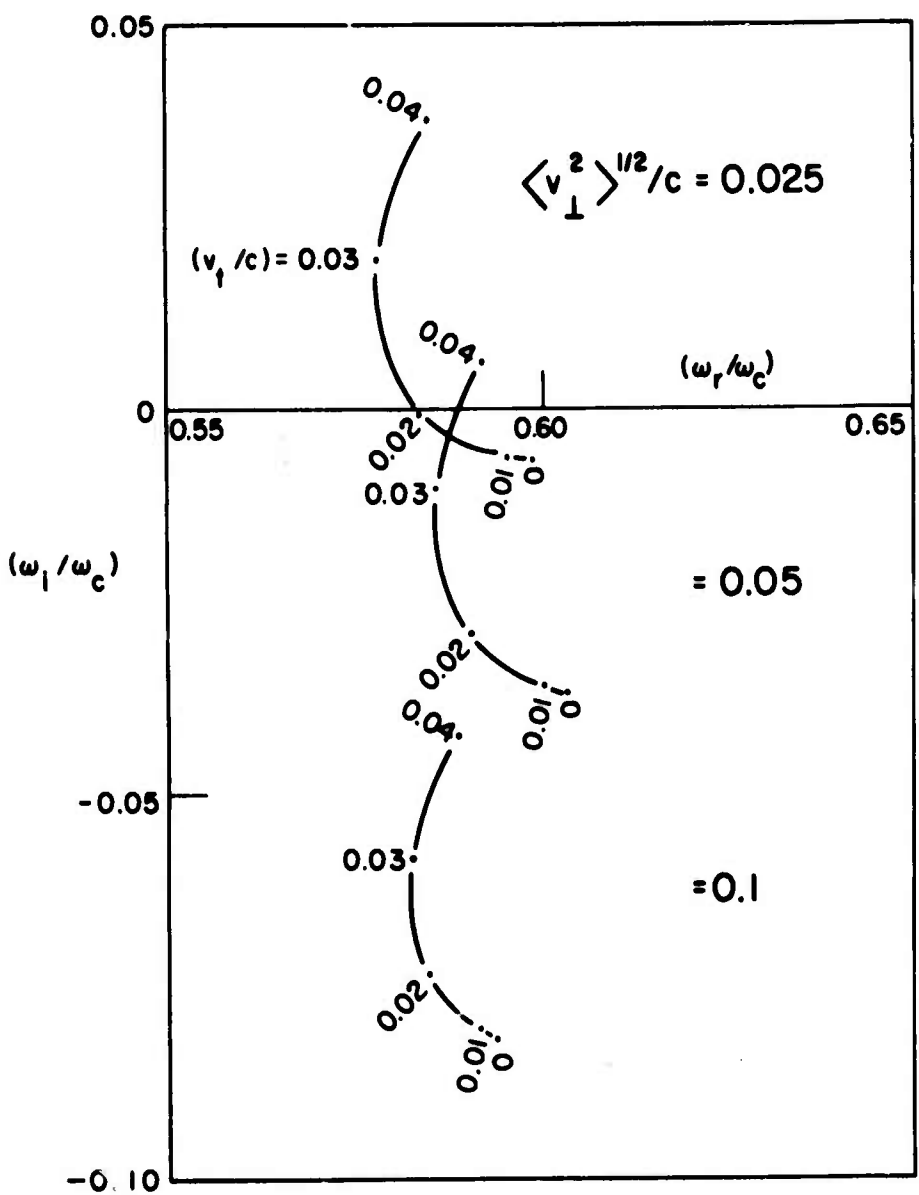


FIG. 9. STABILITY ANALYSIS: EFFECT OF PLASMA TEMPERATURE
 $[(\omega_p^2/\omega_c^2) = 25, (\omega_b^2/\omega_c^2) = 1, (v_{0\parallel}/c) = -0.05]$.

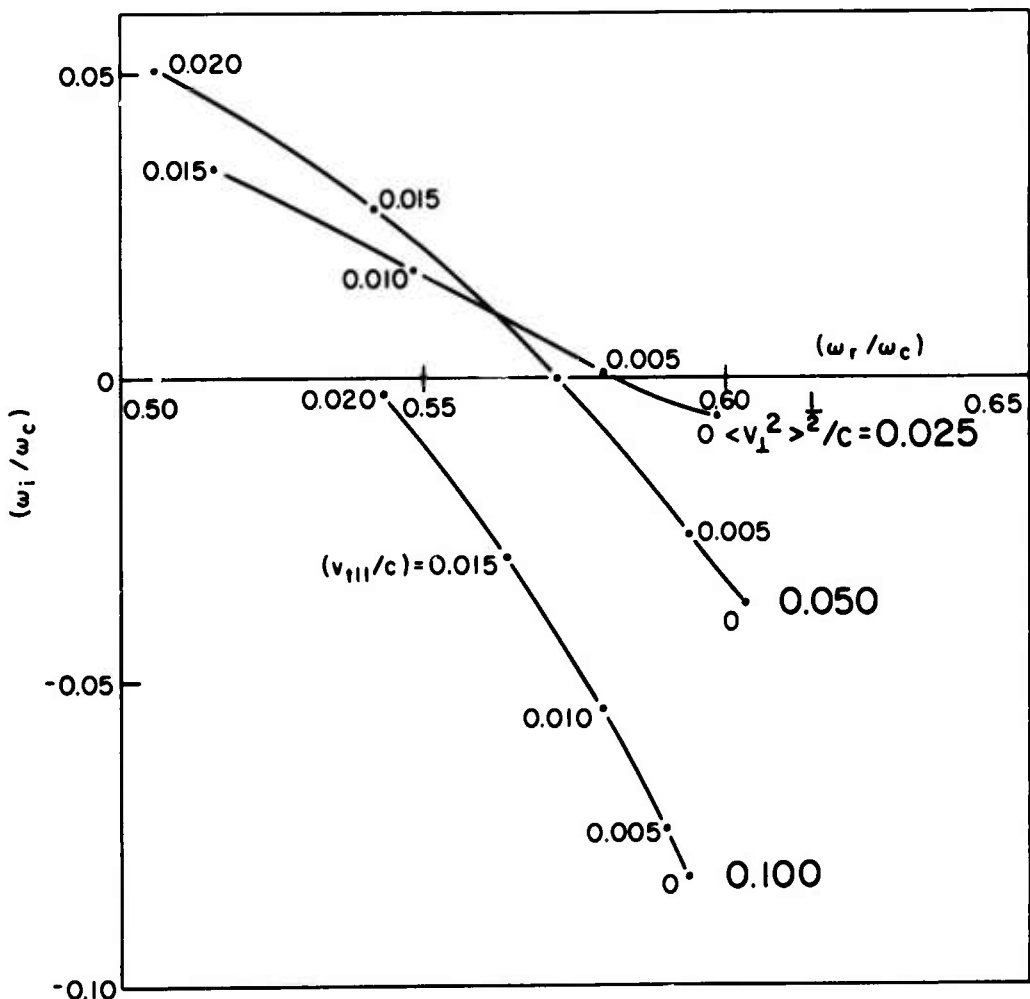


FIG. 10. STABILITY ANALYSIS: EFFECT OF BEAM TEMPERATURE
 $[(\omega_p^2 / \omega_c^2) = 25, (\omega_b^2 / \omega_c^2) = 1, (v_{0\parallel} / c) = -0.05]$.

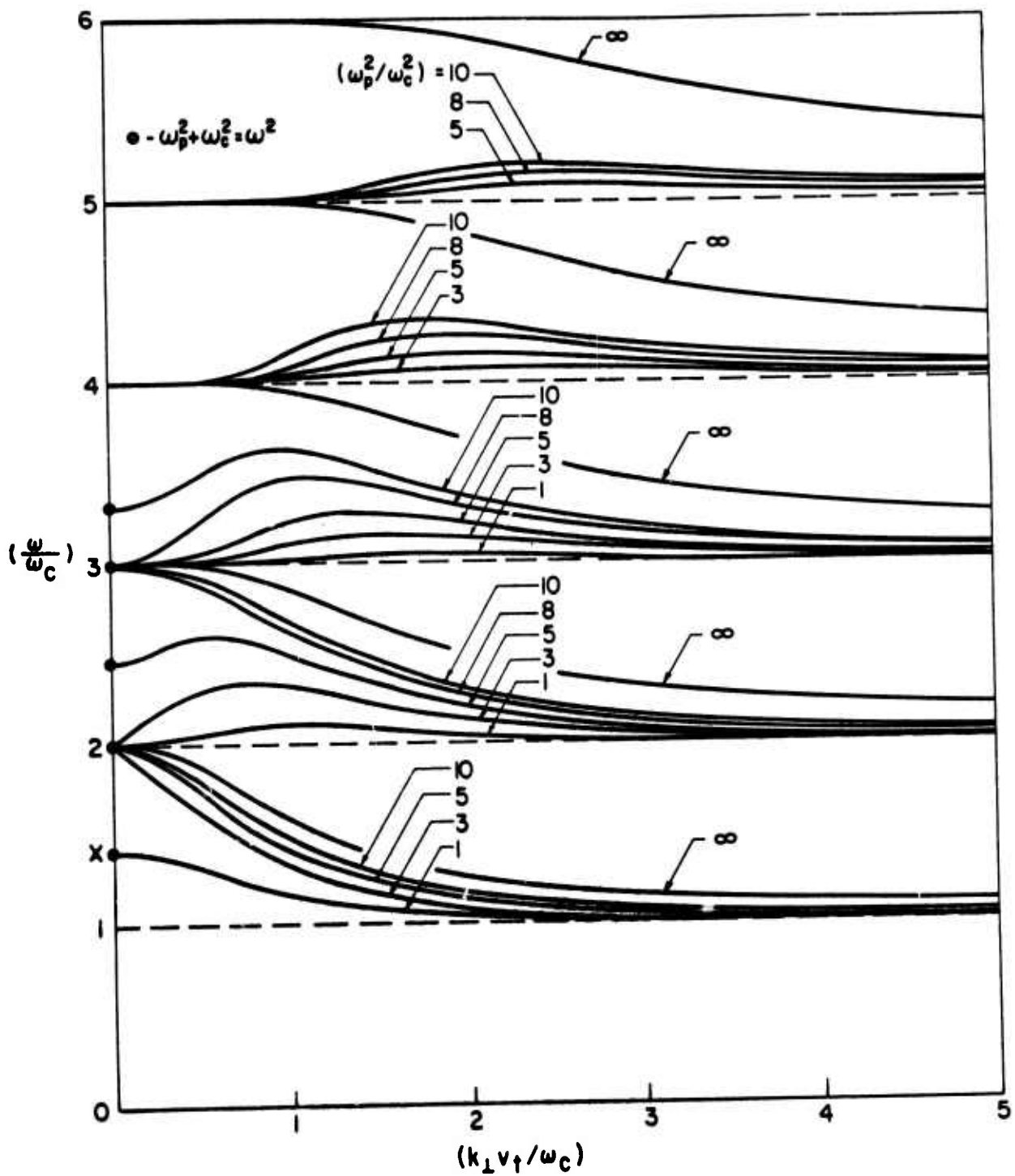


FIG. 11. DISPERSION CHARACTERISTICS FOR PERPENDICULARLY PROPAGATING CYCLOTRON HARMONIC WAVES: MAXWELLIAN ELECTRON VELOCITY DISTRIBUTION.

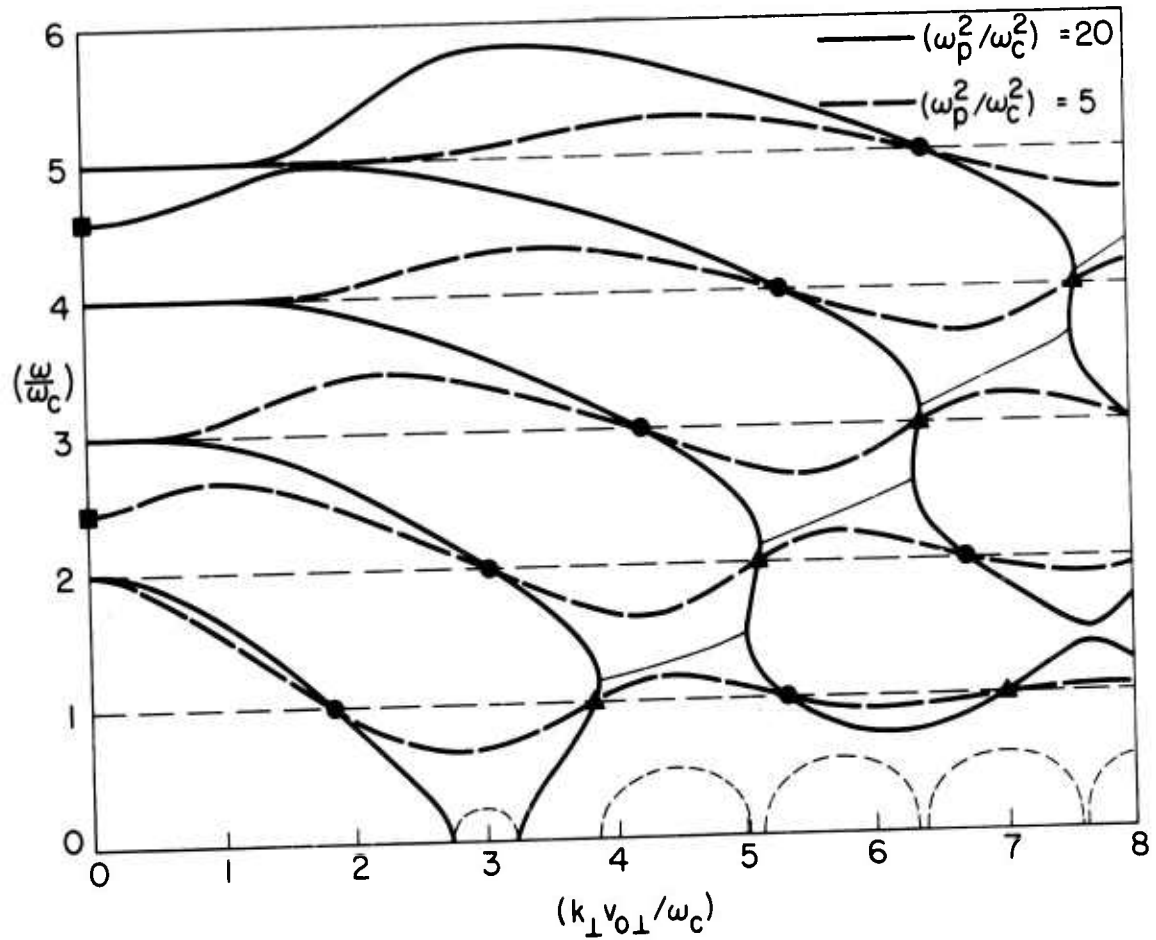


FIG. 12. DISPERSION CHARACTERISTICS FOR PERPENDICULARLY PROPAGATING CYCLOTRON HARMONIC WAVES: RING ELECTRON VELOCITY DISTRIBUTION.

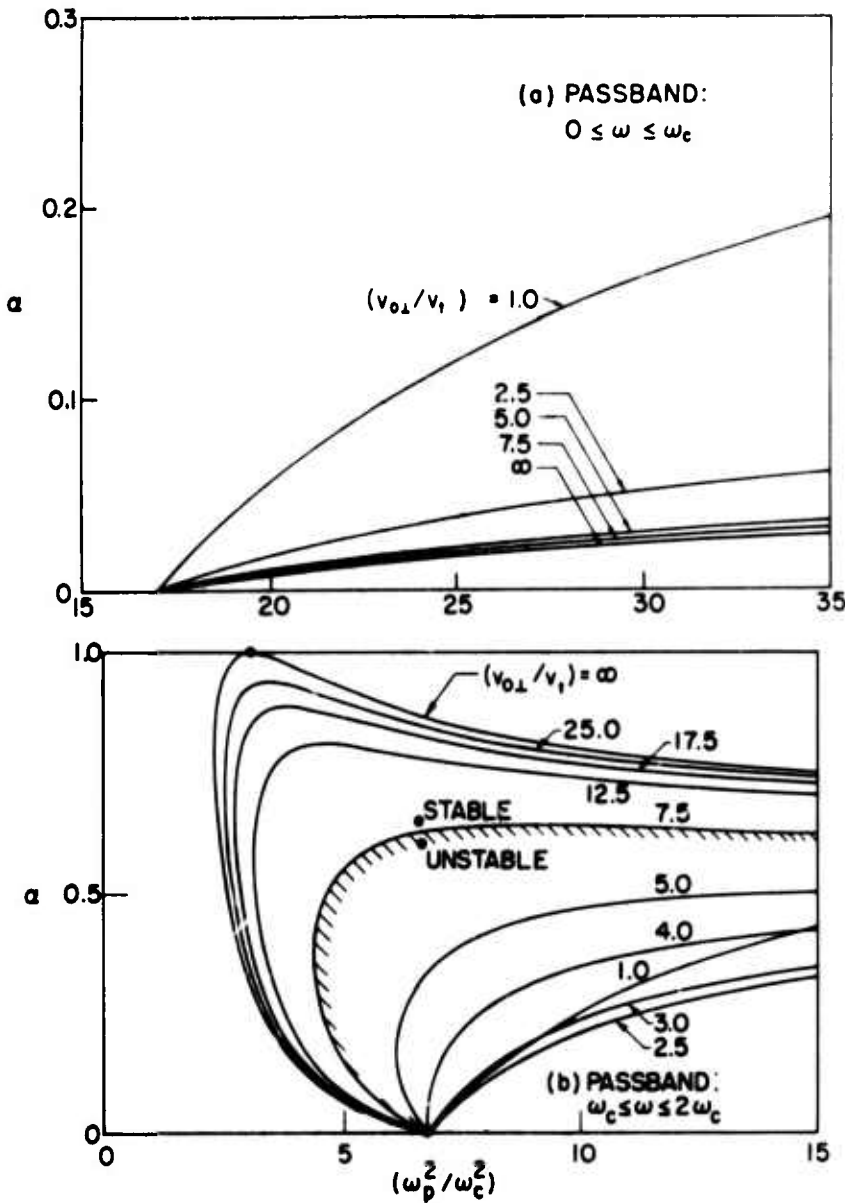


FIG. 13 (a) and (b). CRITERIA FOR THE ONSET OF INSTABILITY FOR PERPENDICULARLY PROPAGATING CYCLOTRON HARMONIC WAVES IN A MIXTURE OF (α) MAXWELLIAN, AND ($1-\alpha$) RING ELECTRON VELOCITY DISTRIBUTIONS.

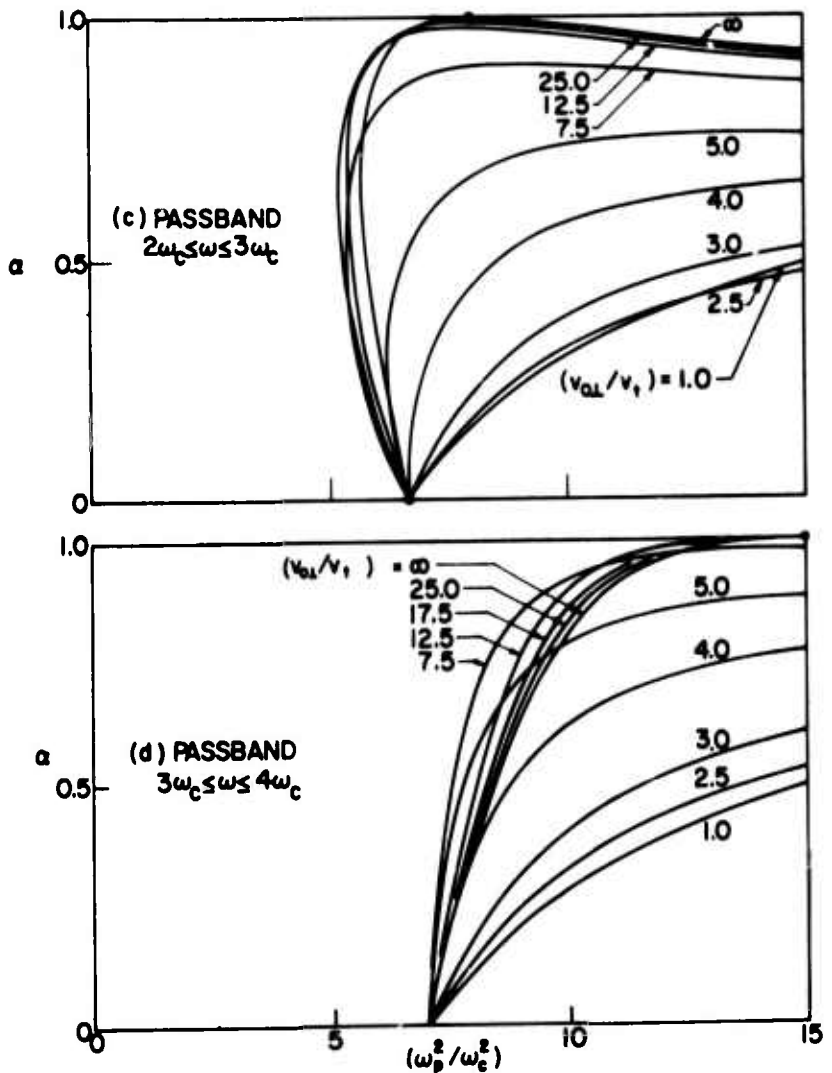


FIG. 13 (c) and (d). CRITERIA FOR THE ONSET OF INSTABILITY FOR PERPENDICULARLY PROPAGATING CYCLOTRON HARMONIC WAVES IN A MIXTURE OF (α) MAXWELLIAN AND ($1-\alpha$) RING ELECTRON VELOCITY DISTRIBUTIONS.

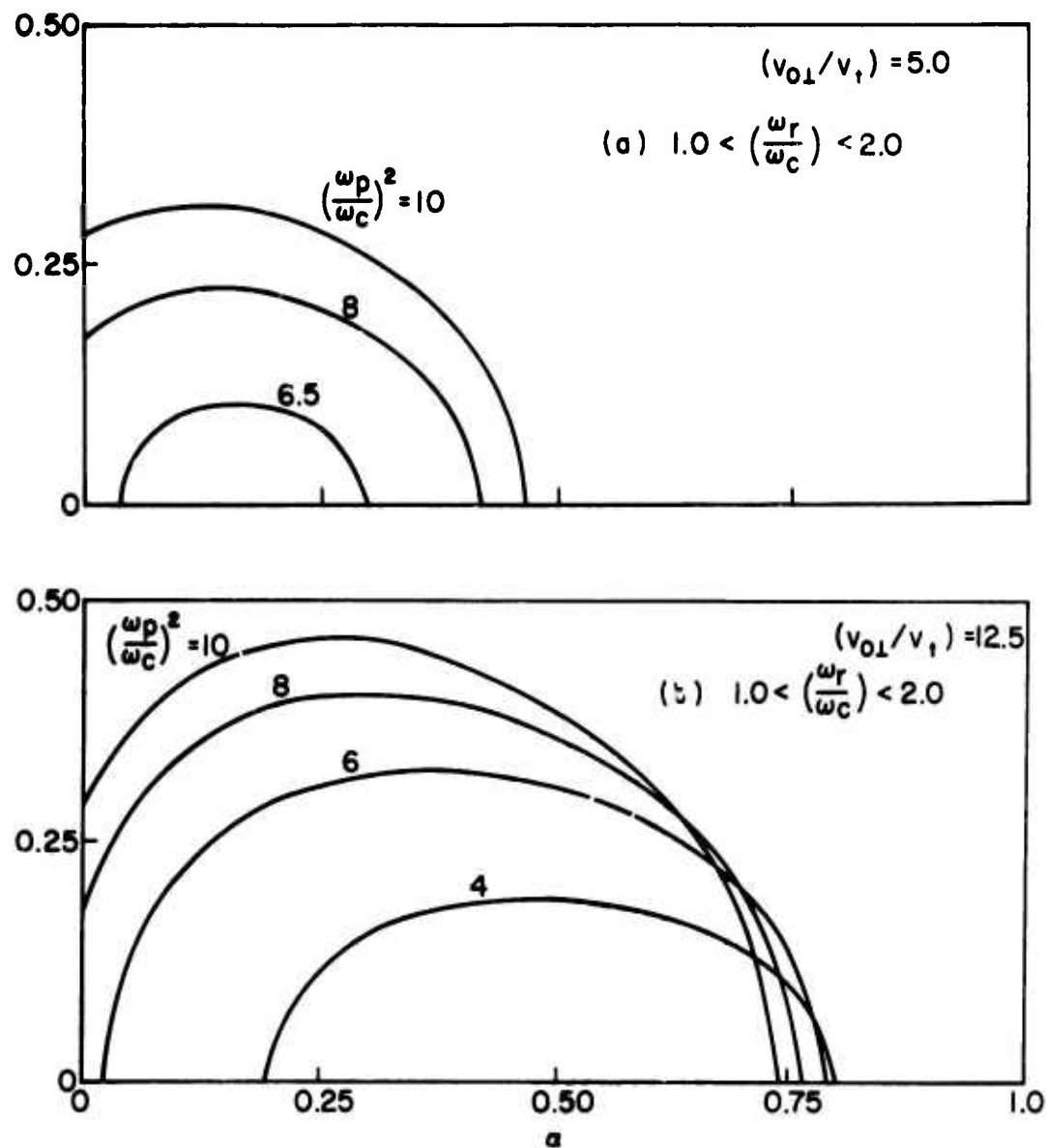


FIG. 14. MAXIMUM INSTABILITY GROWTH RATES FOR A MIXTURE OF MAXWELLIAN AND RING ELECTRON VELOCITY DISTRIBUTIONS.

Security Classification

DOCUMENT CONTROL DATA - R&D

(Security classification of title, body of abstract and indexing annotation must be entered when the overall report is classified)

1. ORIGINATING ACTIVITY (Corporate author) Institute for Plasma Research Stanford University Stanford, California		2d. REPORT SECURITY CLASSIFICATION Unclassified
3. REPORT TITLE SOME STUDIES OF WHISTLER INSTABILITY		2e. GROUP NA
4. DESCRIPTIVE NOTES (Type of report and inclusive dates) Technical Report		
5. AUTHOR(S) (First name, middle initial, last name) F. W. Crawford, J. C. Lee and J. A. Tataronis		
6. REPORT DATE March 1968	7a. TOTAL NO. OF PAGES 40	7b. NO. OF REPS 24
8a. CONTRACT OR GRANT NO DA28-043 AMC-02041(E), ARPA Order No. 605	8c. ORIGINATOR'S REPORT NUMBER (If any) SU-IPR No. 233	
b. PROJECT NO c. 7400.21.243.40.01.50.410.5 d.	8d. OTT OR REPORT NO(S) (Any other numbers that may be assigned this report) ECOM-02041-13	
10. DISTRIBUTION STATEMENT This document is subject to special export controls and each transmittal to foreign governments or foreign nationals may be made only with prior approval of CG, USAECOM, Attn: AMSEL-KL-TG, Ft. Monmouth, N.J. 07703		
11. SUPPLEMENTARY NOTES	12. SPONSORING MILITARY ACTIVITY US Army Electronics Command Ft. Monmouth, N.J. - AMSEL-KL-TG	

13. ABSTRACT

This paper treats the instability excited when a transverse electromagnetic plasma wave, propagating in the right-hand polarized (whistler) mode parallel to a uniform magnetic field, interacts with a stream of monoenergetic gyrating electrons. The objectives of the work are two-fold, first to obtain numerical estimates of the growth rates for various parameters, and second to identify the instabilities as being either absolute or convective. The results show that if the background plasma temperature is zero, absolute instability, i.e. temporal growth, always occurs. This instability may be quenched either by introducing a longitudinal energy spread in the beam. Even when whistler growth is predicted theoretically, it may not be observable in practice, due to the presence of competing instabilities. Two of these are treated in the paper: perpendicularly propagating cyclotron harmonic waves, and longitudinal beam/plasma interaction.

Security Classification

14. KEY WORDS	LINK A		LINK B		LINK C	
	ROLE	WT	ROLE	WT	ROLE	WT
Beam Plasma Interaction						
Whistler Mode Propagation						
Plasmas Instabilities						
Microwave Amplification						